

Tissue Engineering for the Diaphragm and its Various Therapeutic Possibilities – A Systematic Review

Agnes K. Boehm, Karl H. Hillebrandt,* Tomasz Dziodzio, Felix Krenzien, Jens Neudecker, Simone Spuler, Johann Pratschke, Igor M. Sauer,* and Marco N. Andreas

Diaphragmatic impairments exhibit high morbidity as well as mortality while current treatment options remain unsatisfactory. Tissue engineering (TE) approaches have explored the generation of an optimal biocompatible scaffold for diaphragmatic repair through tissue decellularization or de novo construction, with or without the addition of cells. The authors conducted a systematic review on the current state of the art in diaphragmatic tissue engineering (DTE) and found 24 articles eligible for final synthesis. The included approaches studied decellularization-based graft generation (9) and de novo bioscaffold construction (9). Three studies focused on in vitro host-scaffold interaction with synthesized, recellularized grafts (2) and decellularized extracellular matrix scaffolds (1). Another three studies investigated evaluation tools for decellularization efficacy. Among all studies, recellularization is performed in both decellularization-based (4) and de novo generated scaffolds (4). De novo constructed biocomposites as well as decellularized and recellularized scaffolds induced pro-regenerative remodeling and recovery of diaphragmatic function in all examined animal models. Potential therapeutic applications comprise substance defects requiring patch repair, such as congenital diaphragmatic hernia, and functional diseases demanding an entire organ transplant, like muscular dystrophies or dysfunction after prolonged artificial respiration.

the diaphragm exerts a distinct role in several somatic processes such as body posture, cardiac function, lymphatic drainage, anti-reflux barrier and emesis, coughing, and swallowing.^[1–3] The diaphragm's exceptional physiological role in the organism is reflected in its composition of radially aligned myofibers sprouting from a central tendon, forming a dome-shaped, mesothelial-lined flat muscle which is constantly working while being exposed to a varying thoracoabdominal pressure gradient at all times (see **Figure 1**).^[2] Based on its multifunctionality, failure in this skeletal muscle affects the physiology of the whole organism, especially in the fetal developmental period.^[4]

The integrity of the diaphragm muscle may be compromised by congenital defects, like congenital diaphragmatic hernia (CDH) or rare cases of diaphragmatic agenesis. Although mortality rates of CDH, which has a total prevalence of 2.6 cases per 10 000 births, have gradually decreased, they remain at a total of 30% to 60% according to a recent international multicenter, retrospective study.^[5] Other etiologies

of impairment include prolonged artificial respiration, trauma, muscular dystrophies, and carcinogenesis of the pleura, peritoneum, and diaphragm itself.^[6–8]

Morbidity continues to pose multiple serious risks to infants affected by CDH, both on the basis of prenatal lung hypoplasia, persistent pulmonary hypertension, and resultant cardiopul-

1. Background

The diaphragm is a life-sustaining skeletal muscle which has gained increasing interest in regenerative medicine and the field of tissue engineering (TE). Apart from being the main respiratory muscle which takes on 80 % of the work in tidal breathing,

A. K. Boehm, K. H. Hillebrandt, T. Dziodzio, F. Krenzien, J. Neudecker, J. Pratschke, I. M. Sauer, M. N. Andreas
Department of Surgery, Charité – Universitätsmedizin Berlin
Augustenburger Platz 1, 13353 Berlin, Germany
E-mail: karl-herbert.hillebrandt@charite.de; igor.sauer@charite.de

K. H. Hillebrandt, T. Dziodzio, F. Krenzien
Berlin Institute of Health at Charité – Universitätsmedizin Berlin
Charitéplatz 1, 10117 Berlin, Germany
S. Spuler
Muscle Research Unit
Experimental and Clinical Research Center
Charité Universitätsmedizin Berlin and Max-Delbrück-Centrum für
Molekulare Medizin in der Helmholtz-Gemeinschaft
Lindenberger Weg 80, 13125 Berlin, Germany

J. Pratschke, I. M. Sauer
Cluster of Excellence Matters of Activity
Image Space Material funded by the Deutsche Forschungsgemeinschaft (DFG, German Research Foundation) under Germany's Excellence Strategy - EXC 2025 - 390648296
Germany

© 2022 The Authors. *Advanced Therapeutics* published by Wiley-VCH GmbH. This is an open access article under the terms of the Creative Commons Attribution-NonCommercial-NoDerivs License, which permits use and distribution in any medium, provided the original work is properly cited, the use is non-commercial and no modifications or adaptations are made.

DOI: 10.1002/adtp.202100247

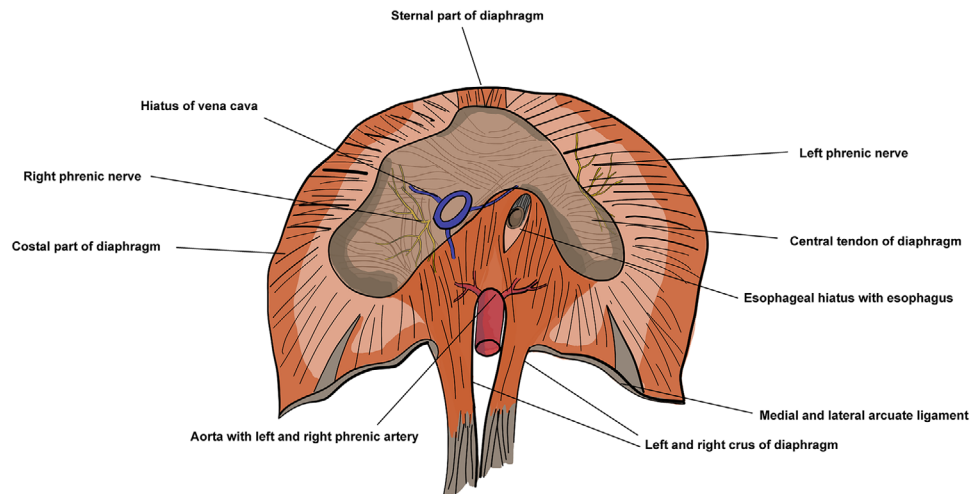


Figure 1. Schematic illustration of diaphragm anatomy.

monary failure, as well as postnatal treatment-associated insufficiencies.^[4,9] These allude to: 1) high recurrence rates; 2) morbidities arising from lack of growth (chest wall deformities in 50% and scoliosis in 27% of cases); and 3) surgical complications like adhesion-induced small bowel obstruction and intraoperative acidosis in thoracoscopic intervention.^[10–16] In muscular dystrophy patients, respiratory muscle weakness—of the diaphragm in particular—is the main cause of morbidity and mortality.^[17,18] Pronounced respiratory dysfunction requires non-invasive or invasive ventilation, which not only leads to an impaired quality of life, but also causes considerable economic expenses with high hospitalization rates and costs due to associated complications.^[18–20] Up to now, there is no treatment for these patients to strengthen the diaphragm to delay or prevent the necessity of ventilation.

With regard to substance defects, conventional treatments differ depending on defect size and underlying condition. In diaphragmatic hernia repair, primary repair (PR) via sutures is preferred, but only feasible in smaller lesions.^[21,22] For larger defects, treatment options include abdominal or thoracic muscle flaps, free fascia lata and pre renal grafts, as well as prosthetic meshes.^[8,10] Patches applied in the clinical setting can be divided based on their original material and degradation behavior into the four main categories of: 1) synthetic non-resorbable (e.g., Gore-Tex [GTX], Marlex, Teflon, Silastic, Dacron); 2) natural resorbable (e.g., porcine small intestinal submucosa; Surgisis [SIS], Permacol, AlloDerm); 3) composite resorbable (e.g., collagen-coated Vicryl mesh); and 4) composite non-resorbable (e.g., Marlex/GTX, Surgisis/GTX, Dacron/GTX), from natural and synthetic base materials, respectively.^[13] Despite their different material-derived properties, multiple retrospective clinical studies reported no significant differences in recurrence rates among non-absorbable meshes (e.g., Dacron and GTX), which amount to 30%, and resorbable scaffolds (e.g., Permacol™ and Surgisis) in infant CDH treatment.^[13,15] Expansion deficiency of nonabsorbable meshes as well as loss of strength owing to rapid degradation in absorbable scaffolds predispose for poor clinical performance.^[3,11,12,21,23]

An ideal prosthesis, which is supposed to be defect-compensating, biomechanically coequal, pro-regenerative, anti-adhesive, non-toxic, low-immunogenic, resistant to infection and enzymatic degradation, easily applicable and available on-demand, should integrate adequately into the host tissue and restore native tissue function while evoking minimum adverse effects.^[3,11,24–26] The two- to threefold cross-sectional expansion of the infant diaphragm sets specific demands for application in congenital defects: a) fast integration; b) the ability to adjust to rapid growth; and c) maintenance of regenerative potential through either an innate stem cell pool or provision of optimal survival conditions for native stem cells.^[15] Establishing a balance between fast degradation and resistance to shear forces and a constant pressure gradient is an additional demand for graft failure prevention. Besides preventing hernia recurrence, minimizing morbidity of patch repair originating from poor growth potential, and pronounced host inflammatory response outlines one of the main objectives addressed by innovative tissue-engineering approaches.

Manifold novel strategies based on de novo scaffold construction and decellularization of allogeneic and xenogeneic tissues or organs, with or without subsequent recellularization, have arisen over the last decade to construct biomaterials suitable for restoration of diaphragmatic function.^[26] Various variables during the development process comprising the choice of underlying base material, construction and processing methods and addition of bioactive components enable fine-tuning of scaffold characteristics, such as immunogenicity, degradability rate, architectural composition, and biomechanical properties.^[26–28] Implanting a scaffold which inheres similar characteristics to the host extracellular matrix (ECM) may provide an ideal foundation for regenerative processes within the scaffold and the surrounding tissue. Effective tissue regeneration is premised on stem cell or progenitor cell invasion, extracellular neo-matrix deposition and—in the best case—deposition of native tissue-resembling matrix with coequal functionality.^[29,30] Sufficient vascularization for oxygen and nutrient supply, tissue homeostasis and immune functions embodies another integral factor to guarantee tissue

maintenance and regeneration.^[13,31] Inadequately prepared ECM scaffolds with cellular residues and immunogenic synthetic composites provoke an intense inflammatory host foreign body reaction (FBR), which predisposes for chronic inflammation and scar tissue formation.^[29,30] Reduction of patch-repair associated morbidities and thus improvement of long-term outcomes is a main rationale for engineering a bioscaffold that successfully overcomes these challenges.

2. Results

Out of 56 eligible studies spanning the last ten years (dated back from the 25th June 2021), 32 were excluded due to not meeting the inclusion criteria as mentioned above and a total of 24 studies were included in the final synthesis (Table 1). The selection process from identification of studies to inclusion in final synthesis is depicted in Figure 2. From those 24 studies, 12 based their studies on decellularized diaphragmatic (DD) tissue. Eight studies investigated different stages of decellularized extracellular matrix (dECM) tissue treatment, processing, facultative recellularization, and implantation. Three studies investigated decellularization efficiency qualitatively and quantitatively, one study assessed in vivo reaction to decellularized matrices. De novo biocomposites were studied by 12 approaches, from which 10 studies reported on their construction and performance. One study focused on evoked cellular response to subcutaneously implanted stem cell seeded matrices while another assessed stem cell viability on different scaffold types.

All studies with two separate treatment arms were appraised for risk of bias (Figure 3).

2.1. Decellularization-Based Scaffolds

The method of decellularization has been employed for various tissues, organoids, and whole organs from the dermal, respiratory, cardiovascular to musculoskeletal system.^[26,32–34] Decellularization of pre-existing tissues constitutes an attractive TE approach as the complex network of ECM remains intact while cellular components are removed. Whereas the processed tissue retains its macro- and ultrastructure, matrix and basement membrane proteins and even growth factors can be preserved depending on the applied decellularization technique.^[32] Removal of cellular components is realized by the sole application or a combination of physical, chemical, and enzymatic methods.^[35,36] However, thorough decellularization often runs at the expense of ECM preservation as harsh processing methods and substances may cause ECM component reduction, disruption, and loss.^[33,37] The balance between thoroughness of cell removal and preservation of ECM components depends on adjustable processing parameters, including type of detergent and time of exposure. Shorter exposure for ECM preservation can be counterbalanced by elevated perfusion pressure to ensure cell removal in perfusion-based approaches.^[33,38] Subsequent to decellularization, tissues can undergo supplementary in vitro manufacturing, for instance processing to hydrogels or crosslinking, or be directly implanted onto the recipient structure.^[36] Constructive in vivo tissue remodeling of the dECM-derived scaffolds depends on processing determinants, such as: a) thorough decellularization; b) a suitable

amount of chemical crosslinking; and c) the absence of microbial contamination.^[39,40] The prosthetic should ideally be applied in an intact microenvironment with adequate mechanical stress stimuli.^[29,30]

2.2. Decellularization Methods for Diaphragmatic Tissue

Engineering of acellular matrices via detergent enzymatic treatment (DET) constitutes the most established method for diaphragmatic decellularization.^[11,31,36,41,42] Cellular material is eroded through repetitive cyclic exposure to detergent substances like the tensides sodium dodecyl sulfate (SDS), sodium deoxycholate (SDC), ethylenediaminetetraacetic acid (EDTA), tri(n-butyl)phosphate (TnBP), and Octoxinol 9 (Triton X-100), most often followed by an enzymatic step with DNase and rinsed with deionized water. Optimal cycle duration and periodicity depend on tissue density and size. In the first implantation approach of donated human hemi-diaphragms in a canine model, 25 DET cycles lasting almost 60 days were necessary to ensure proper decellularization.^[24] In comparison, cycle duration for murine diaphragms usually ranges from 1 to 4 cycles lasting ≈ 1 to ≈ 3 days. DET is most commonly applied via continuous agitation on an orbital shaker,^[9,38] whereas retrograde perfusion through the inferior vena cava combined with standard agitation is feasible as well.^[11] Physical freeze-and-thaw-based decellularization with three cycles of freezing at -80 °C followed by thawing for 15 min proved unsuitable for the diaphragm, completely destructing its ECM network.^[37] Various decellularization protocols for DTE in the last ten years are listed in Table 2.

2.3. Pre-Implantation Evaluation Tools for Decellularization-Based Grafts

Quality criteria for decellularization efficiency are set upon: a) a residual DNA concentration of less than 50 ng dsDNA per mg ECM dry weight; b) a maximum DNA fragment size of 200 bp; and c) negative histology for nuclear material in tissues stained with 4',6-diamidino-2-phenylindole (DAPI) or hematoxylin and eosin (H&E).^[32,43] DNA quantification can be performed using DNA quantification kits followed by spectrophotometric analysis.^[11,41,42] Evaluation of decellularization efficiency in dECM grafts is usually realized through semi-quantitative histological assessment.^[9–11,24,31,37,41,42] Aside from qualitative assessment, quantitative measurement methods are key to establishing defined standards for decellularization efficacy. Additional non-invasiveness is favorable as it enables qualitative scanning for every individual graft without its destruction for histological preparation. The *Krasnodar group* has recently examined both quantitative and qualitative non-invasive evaluation tools for verification of decellularization efficiency.^[11,35,44,45] Accordingly: 1) quantitative determination of cell viability through electron paramagnetic resonance spectroscopy; and 2) monitoring free radical generation through chemiluminescence may serve as objective decellularization quantification tools. Ultrasound imaging as a clinically proven safe examination method can likewise be employed for decellularized, as well as recellularized tissues through high-frequency acoustic microscopy prior to implanta-

Table 1. All studies included in this systematic review.

Year	Work group	Publication	Animal model (population, age, animal, breed, weight)	Surgical defect	Tissue engineering method	Group allocation	Follow-up time	Survival	Complications
2013	Brouwer et al.	Collagen-Vicryl Scaffolds for Reconstruction of the Diaphragm in a Large Animal Model	(n = 9) 11 to 24 d lambs (Texel/Flevoiland breed)	3 cm × 1.5 cm posterolateral diaphragmatic defect (at musculotendinous interface)	Incubation of Vicryl sheets in collagen suspension; EDC/NHS crosslinking	1) Col-Vicryl-HGF 1 scaffold; 2) Col-Vicryl scaffold; 3) CTRL (not operated)	4 weeks, 6 months	89%	(n = 1; group 2) lower motor neuron failure; eventrations in all cases
2013	Brouwer et al.	Construction and In Vivo Evaluation of a dual Layered Collagenous Scaffold with a Radial Pore Structure for Repair of the Diaphragm	(n = 8) male rats (Wistar; 230–250 g)	Ø 1.2 cm right diaphragmatic defect (muscular diaphragm)	Compressed collagen bottom layer and top radial pore scaffold; EDC/NHS crosslinking	1) Crosslinked radial collagen scaffold; 2) control crosslinked random poured porous collagen scaffolds	12 weeks	100%	(n = 1) partial liver herniation; adhesions in all animals
2012	Brouwer et al.	Repair of Surgically Created Diaphragmatic Defect in Rat with Use of a Crosslinked Porous Collagen Scaffold	(n = 25) male rats (Wistar; 230–250g)	Ø 1.2 cm right diaphragmatic defect	EDC/NHS-crosslinked porous type I collagen scaffold	5 same-procedure groups with different follow-up time points	2 weeks, 3 weeks, 8 weeks, 12 weeks, 24 weeks	88%	(n = 2 anesthesia intolerance; n = 1 illness of unknown aetiology); adhesions in all animals
2013	Brouwer et al.	Heparinized Collagen Scaffolds with and without Growth Factors for the Repair of Diaphragmatic Hernia	(n = 36) male rats (Wistar; 230–250 g)	Ø 1.2 cm right diaphragmatic defect	Covalent binding of heparin ± VEGF ± HGF	1) Col-Hep; 2) Col-Hep-V; 3) Col-Hep-H; 4) Col-Hep-VH; 5) Col-X	2 weeks, 12 weeks	100%	Liver adhesions in all animals
2015	Piccoli et al.	Improvement of Diaphragmatic Performance through Orthotopic Application of Decellularized Extracellular Matrix Patch	Donors and OTX: 8–12 weeks male and female C57BL/6j mice (wt.); host atrophic model: 3 months HSA-Cre; Smn ^{fl/fl} /F7	Atrophic model: mounting of 3 mm × 5 mm dECM patch	DET	1) Intervention group; 2) CTRL group (untreated control, 0 d)	4 d, 7 d, 15 d, 30 d, 90 d	n/a	Liver adhesions
2018	Fallas et al.	Decellularized Diaphragmatic Muscle Drives A Constructive Angiogenic Response In Vivo	Donors and OTX: (n = 8) 12 weeks male and female C57BL/6j mice (B6); subcutaneous implantation: 12 weeks male and female B6 UBC-GFP mice (GFP+)	Orthotopic (left hemidiaphragm) and subcutaneous implantation of dECM patches (not specified)	DET	1) DD groups; 2) ePTFE (CTRL)	7 d, 15 d	n/a	n/a

(Continued)

Table 1. (Continued).

Year	Work group	Publication	Animal model (population, age, animal, breed, weight)	Surgical defect	Tissue engineering method	Group allocation	Follow-up time	Survival	Complications
2019	Trevisan et al.	Generation of a Functioning and Self-Renewing Diaphragmatic Muscle Construct	3 months C57/BL/6j mice	Not given	DET; seeding of dECM patches; exploration of 5 different storage conditions for dECM	1) Fresh; 2) 2w4C; 3) 2m4C; 4) 2wLN; 5) 2mLN	4 d, 7 d, 12 d, 21 d	n/a	n/a
2019	Trevisan et al.	Allogenic Tissue-Specific Decellularized Scaffolds Promote Long-Term Muscle Innervation and Functional Recovery in a Surgical Diaphragmatic Hernia Model	Donors: 12 weeks C57BL/6j male and female mice; recipients: (<i>n</i> = 78) 12 weeks BALB/c male and female; further analysis: (<i>n</i> = 9) GFP+Schwann cell mouse model	3 mm × 5 mm left hemi-diaphragmatic defect	DET	1) DD groups; 2) ePTE (CTRL); 3) healthy untreated	2 d, 5 d, 15 d, 30 d, 90 d	Surgery survival rate 64%; follow-up survival rate: DD 57% versus ePTE 46%	ePTE-treated: liver herniation in 20%, fibrotic encapsulation in all cases
2021	Boso et al.	Porcine Decellularized Diaphragm Hydrogel: A New Option for Skeletal Muscle Malformations	Donors: (<i>n</i> = 7) mice (unspecified); recipients: (<i>n</i> = 6) BALB/c Rag2 ^{-/-} /γc ^{-/-} mice	3 mm × 5 mm left hemi-diaphragmatic defect	DET-treated porcine ECM hydrogel preparation with gelation and genipin-crosslinking	1) Crosslinked compared; 2) non-crosslinked hydrogels	3 d, 7 d	n/a	None
2015	Gubareva et al.	Orthotopic Transplantation of a Tissue Engineered Diaphragm in Rats	Donors: (<i>n</i> = 97) 8 weeks male rats (Lewis; 250 ± 50 g); recipients: OTX (<i>n</i> = 15) adult male rats	En bloc diaphragm explantation, Dorsal subcutaneous allogeneic transplantation (DSAT); orthotopic re-transplantation	DET; seeding of rat BM-MSCs	DSAT: 1) sham; 2) ND implant; 3) DD implant; OTX: 1) CTRL (normal, untreated); 2) sham (autologous re-implantation of a priori resected left HD); 3) treated (resection + implantation reseeded scaffold)	7 d, 21 d, 3 weeks	100%	Adhesions to liver (<i>n</i> = 2)

(Continued)

Table 1. (Continued).

Year	Work group	Publication	Animal model (population, age, animal, breed, weight)	Surgical defect	Tissue engineering method	Group allocation	Follow-up time	Survival	Complications
2016	Gubareva et al.	EPR Spectroscopy Solutions for Assessment of Decellularization of Intrathoracic Organs and Tissues	(n = 25) outbred male rats (200 g ± 50 g)	Assessment of heart-lungs-complex and diaphragm	DET	None	None	n/a	n/a
2018	Sotnichenko et al.	Morphological Evaluation of the Tissue Reaction to Subcutaneous Implantation of Decellularized Matrices	(n = 20) male rats (Wistar; 210 ± 40 g)	Subcutaneous implantation (interscapular region) of dECM (lung, heart, diaphragm) and assessment	DET	1) Lung; 2) diaphragm; 3) heart	7 d, 14 d	n/a	n/a
2019	Gubareva et al.	Estimation of Decellularization and Recellularization Quality of Tissue-Engineered Constructions by the Chemiluminescence Method	None	(Pre-prepared)	DET	None	None	n/a	n/a
2019	Morokov et al.	Noninvasive Ultrasound Imaging for Assessment of Intact Microstructure of Extracellular Matrix in Tissue Engineering	(n = 3) adult male rats (Wistar; 220 ± 50 g)	(Pre-prepared)	DET	1) ND; 2) DD; 3) collagenized diaphragm; 4) native lung; 5) decell lung	None	n/a	n/a
2017	Lesage et al.	Modulation of the Early Host Response to Electrospun Poly(lactic Acid) Matrices by Mesenchymal Stem Cells from the Amniotic Fluid	3 months male rats (Wistar)	Subcutaneous pouch; en bloc harvest of original implant area and underlying abdominal wall structures	Electrospun PLA scaffold seeded with AF-MSCs	1) AF-MSCs; 2) AF-MSCs CTRL; 3) FB-seeded matrix; 4) FB CTRL	14 d	n/a	None
2018	Eastwood et al.	Testing Novel Scaffolds for Diaphragmatic Hernia Repair	(n = 41) 6 weeks male rabbits (New Zealand White; ca. 1.5 kg)	3 cm x 3 cm left posterior diaphragmatic defect	RP-Composite assembly via crosslinking radial pore oriented type I collagen and 4-ply SIS	1) Gore-Tex; 2) RP-Composite; 3) SIS; 4) sham (abdominal packing)	60 d, 90 d	Overall 76% in early post-operative period (10 deaths unrelated to scaffolds; n = 4 pneumothorax; n = 3 unable to maintain airway post-extubation, n = 1 death in recovery (<2 h), n = 1 no identified cause [3 d])	Reherniation or eventrations: Gore-Tex 17%, RP-Composite 22%; SIS 100%; adhesions assessed by score (scar, mesh, left lung); (n = 2) delamination in RPC

(Continued)

Table 1. (Continued).

Year	Work group	Publication	Animal model (population, age, animal, breed, weight)	Surgical defect	Tissue engineering method	Group allocation	Follow-up time	Survival	Complications
2013	Zhao et al.	Diaphragmatic Muscle Reconstruction with an Aligned Electrospun Poly(ϵ -caprolactone)/collagen hybrid scaffold	(<i>n</i> = 52) 14 weeks female rats (Lewis)	2 cm × 3cm central left hemi-diaphragmatic defect	Aligned, crosslinked electrospun PCL/collagen hybrid scaffold via electrospraying	1) PLC/CSC; 2) CTRL (sham)	1 month, 2 months, 3 months, 6 months	100%	Liver adhesions in 5/23 animals in scaffold implant group
2016	Davari et al.	Partial Replacement of Left Hemidiaphragm in Dogs by Either Cryopreserved or Decellularized Heterograft Patch	(<i>n</i> = 11) adult male and female dogs (clinical mix-bred, 20 ± 2 kg)	Deceased human donor en bloc left hemi-diaphragm retrieval and canine native diaphragm replacement	Cryopreservation versus DET	1) untreated diaphragm; 2) DD	3 weeks, 6 months	100%	Patch motion impairment in all cases; group 1 (3 weeks post-OP): mild atelectasis, scattered infiltration in the left lower lobe, fibrotic bands, and minimal fluid collection; group 2 (6 months post-OP): mild/moderate diaphragmatic elevation, adhesions
2017	Suzuki et al.	Engineering and Repair of Diaphragm Using Biosheet (A Collagenous Connective Tissue Membrane) in Rabbits	Donors: female rabbits (New Zealand white; 0.7–1.0 kg); OTX: female rabbits (New Zealand white; 1.5–2.7 kg)	1.5 cm × 1.5 cm left hemi-diaphragmatic defect	Formation of autologous biosheet via subcutaneous silicone mold implantation	1) Core-Tex Soft Tissue Patches; 2) Seamdura; 3) autologous two-ply biosheets	4 weeks, 12 weeks	100%	Incidence of liver herniation: 1) 45%; 2) 73%; 3) 21%
2017	Liao et al.	Tissue Engineering to Repair Diaphragmatic Defect in Rat Model	Donors OTX: rats (no details given); donors (biomechanical testing): (<i>n</i> = 6) 7–8 weeks female rats (Sprague Dawley; 150–175 g; recipients OTX: (<i>n</i> = 40), 7 weeks female rats (Sprague Dawley; 150–175 g)	1.2 cm × 1.2 cm left diaphragmatic defect (75% tendon, 25% muscle)	Recolonization of DET-prepared dECM with hAF-MSCs	1) hAF-MSCs seeded decel scaffolds; 2) DD; autologous control	4 months, 6 months	n/a	None

(Continued)

Table 1. (Continued).

Year	Work group	Publication	Animal model (population, age, animal, breed, weight)	Surgical defect	Tissue engineering method	Group allocation	Follow-up time	Survival	Complications
2017	Shieh et al.	Comparisons of Human Amniotic Mesenchymal Stem Cell Viability in FDA-Approved Collagen-Based Scaffolds: Implications for Engineered Diaphragmatic Replacement	None	None	AF-MSCs seeding of 2 different collagen-based scaffolds	1) VitroCol; 2) SurgiMend	1, 3, 5 d	n/a	n/a
2018	Zhang et al.	Regeneration of Diaphragm with Bio-3D Cellular Patch	8–12 weeks male rats (F344/N-rnu)	1.2 × 1.0 mm rectangular left-diaphragmatic defect	Construction of scaffold-free tubular tissue from MCS via 3D-printing (Kenzan method) HDF (90%) and HUVECs (10%); bioreactor with tidal currents culture	1) No repair; 2) Vicryl mesh repair; 3) cellular patch repair	2 weeks, 3 weeks, 1 month, 4 months, 7 months, 10 months	1) 0%; 2) 17% 3) 100%	Liver herniation
2020	Arai et al.	Cryopreservation Method for Spheroids and Fabrication of Scaffold-Free Tubular Constructs	None	None	Cryopreservation of fibroblast cell-based spheroids, fusion of spheroids post-thawing	1) Cryopreservation; 2) non-cryopreservation	14 d, 21 d, 28 d	n/a	n/a
2018	Sesil et al.	Decellularization of Rat Adipose Tissue, Diaphragm, and Heart: A Comparison of Two Decellularization Methods	Donors: (n = 5) male albino rats (Wistar; 250–300 g); Ad-MSCs harvest: (n = 2) male albino rats (Wistar; 250–300 g)	Sterile resection of diaphragm (not specified)	Comparison of decellularization method A (DET) and method B (freeze-and-thaw)	1) Decell method A; 2) decell method B	1 d, 2 d, 3 d	n/a	n/a

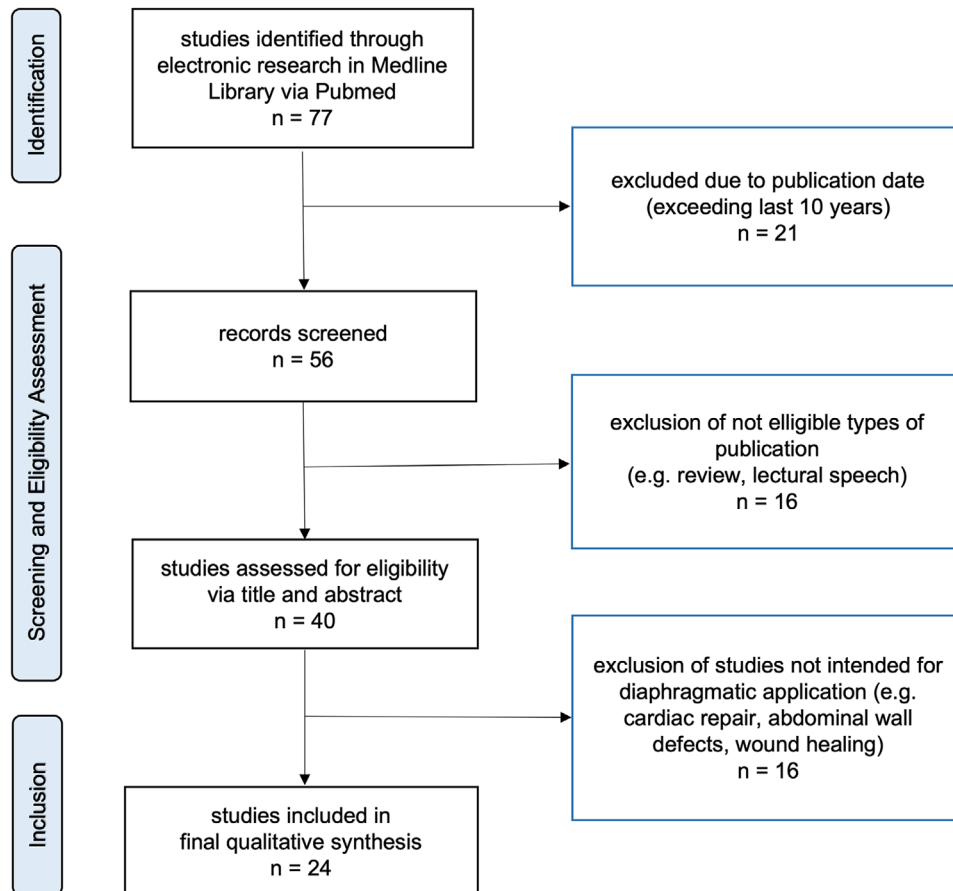


Figure 2. Selection process for study inclusion into systematic review. From initially 77 identified studies from data bases, 24 studies were finally included into synthesis.

tion. This could especially benefit evaluation of growing and regenerating tissues with a high turnover, as those are particularly sensitive to detrimental radiation from conventional visualization techniques (e.g., X-ray, computer tomography).^[44]

2.3.1. Properties and In Vivo Performance of dECM Scaffolds

Decellularized grafts emulate native tissue function by exhibiting biomechanical resistance and morphologically functional performance when implanted.^[11] Depending on thoroughness of cell residue removal, dECM matrices are low-[31] to non-immunogenic.^[11] The induced host alloresponse differs from that of synthetic patches regarding cell invasion, tissue integration, myogenic induction, and angiogenic and neural response.^[10,31,46] Accordingly, limited adverse^[11] and even positive inflammatory response^[43] carried by a macrophage polarization switch characterizes the pro-regenerative environment created upon dECM scaffold implantation. DD ECM grafts can secure long-lasting angiogenic stimuli as fundament for successful angiogenesis.^[10,31] Their pro-angiogenic potential is based on the preservation of angiogenic cytokines like vascular endothelial growth factor (VEGF) and angiopoietin, matrikines and endothelialization enzymes (e.g., endothelin), and metalloproteases

(e.g., matrix metalloproteinase 9) which stimulate new vessel formation within the implanted dECM patch.^[31] Tissue regeneration with angiogenesis was seen to be more pronounced in dECM treated diaphragms than upon expanded polytetrafluoroethylene (ePTFE) application, which evokes clear FBR, aggravation of inflammation and lack of cell migration.^[31] Decellularized grafts are capable of inducing muscle tissue regeneration by myofiber ingrowth from the surrounding tissue and new muscle fiber generation. Activation and migration of satellite cells,^[43] initial fusion of myogenic progenitor cells and significantly upregulated markers for muscle fiber regeneration characterize this myoregenerative state.^[10] The expression of embryonic myosin heavy chain Myh3 positive fibers combined with increased muscle thickness indicates the presence of newly synthesized muscle.^[41] One study suggests that although early post-injury responses of the muscle self-regenerating properties can be independent of patch material (dECM versus ePTFE), the distinguishable feature of dECM-treated scaffolds is securing a prolonged pro-myoregenerative state.^[10] In-depth functional muscle regeneration is accomplished when not only muscular structures are reforming, but neuronal connectivity is reestablished as the basis for active contraction rather than merely passive comovement. Complete fusion of dECM-patches with the native diaphragmatic environment was confirmed by Schwann cell in-

Random Sequence Generation (selection bias)
Group Comparability and Confounders
Allocation concealment (selection bias)
Random animal housing
Blinding of participants and personnel (performance bias)
Animal assessment for outcome
Blinding of outcome assessment (detection bias)
Incomplete outcome data (attrition bias)
Selective reporting (selection bias)
Other bias

Arai et al. 2020	x	?	x	n/a	x	n/a	x	✓	✓	?
Boso et al. 2021	x	x	x	n/a	x	n/a	x	x	✓	x
Brouwer et al. May 2012	x	✓	x	x	x	x	x	✓	✓	?
Brouwer et al. Mar 2013	x	✓	x	x	x	x	x	x	✓	?
Brouwer et al. 2013	x	✓	x	x	x	x	x	x	✓	?
Brouwer et al. Oct 2013	x	?	x	✓	x	x	x	✓	✓	x
Davari et al. 2016	x	x	x	x	x	x	x	✓	✓	x
Eastwood et al. 2018	✓	✓	✓	x	✓	x	✓	✓	✓	x
Fallas et al. 2018	x	✓	x	x	x	x	✓	✓	✓	?
Gubareva et al. 2015	x	✓	x	x	x	x	x	✓	✓	?
Gubareva et al. 2016	n/a	n/a	n/a	n/a	n/a	n/a	n/a	n/a	n/a	n/a
Gubareva et al. 2019	n/a	n/a	n/a	n/a	n/a	n/a	n/a	n/a	n/a	n/a
Lesage et al. 2017	✓	x	✓	x	x	x	✓	✓	✓	?
Liao et al. 2017	x	✓	x	x	x	x	x	✓	✓	?
Morokov et al. 2019	x	✓	x	x	x	x	x	✓	✓	?
Piccoli et al. 2015	x	✓	x	x	x	x	✓	✓	✓	?
Sesli et al. 2018	x	x	x	x	x	x	x	✓	✓	x
Shieh et al. 2017	x	✓	x	n/a	x	n/a	x	✓	✓	?
Sotnichenko et al. 2018	n/a	n/a	n/a	n/a	n/a	n/a	n/a	n/a	n/a	n/a
Suzuki et al. 2017	x	x	x	x	x	x	x	✓	✓	?
Trevisan et al. Mar 2019	x	✓	x	x	x	x	✓	x	✓	?
Trevisan et al. Apr 2019	x	✓	x	x	x	x	x	✓	✓	x
Zhang et al. 2018	✓	x	✓	✓	✓	✓	✓	x	✓	?
Zhao et al. 2013	x	x	x	x	x	x	x	✓	✓	?

filtration and the presence of functional neuromuscular junctions (confirmed via α -bungarotoxin staining), for which ePTFE-treated controls were negative.^[41] In dECM-treated specimens, morphological contractibility of the reconstructed diaphragmatic muscle was validated via phrenic nerve hemidiaphragm assay by electrical stimulation of both preserved phrenic nerves.^[10]

2.4. De Novo Generated Biocomposites

The appeal of grafting a biocompatible scaffold de novo not only lies in the possibility to initially calculate and implement bio- and physicomaterial requirements for the composite, but also in evading the necessity of a one-on-one donor organ as opposed to whole tissue decellularization concepts. Base materials of organic nature, such as donated animal-derived or human tissues, and synthetic polymers can be manufactured by numerous techniques including 3D printing,^[49] electrospinning,^[3,22] liquid nitrogen freezing,^[27] and multilayering via compression assembly,^[50] and optionally further processed for specific qualities.^[21,36,47]

Regaining complete diaphragmatic tissue functionality in large defects is based on the presence of muscle cells, which can be realized through promoting ingrowth from the surrounding tissue or providing optimal conditions for growth originating from either in vitro or in vivo recolonized stem cells. As opposed to—particularly skeletal-muscle-derived—dECM scaffolds, de novo constructed meshes do not inherently hold bioactive factors and the naturally assimilated extracellular network for optimal skeletal muscle cell function and growth. Manufacturing methods may optimize the prosthetic's features to facilitate myoregenerative processes by emulation of the native ECM. The ECM synthesized by its resident cells provides them an optimal microenvironment, and thus rebuilt should attract, nourish, and replenish new resident cells to form their original tissue in the best way possible. Variations of scaffold pore size and fiber alignment through liquid nitrogen freezing have shown to create a radial fiber alignment similar to native diaphragm (ND) structure.^[27] Further constructional parameters to authentically mimic the macroscopic ND muscle include 3D shape (dome/cone shape versus flat) and structural layering of pleural-mesothelium, muscle, and peritoneal-mesothelium.

2.5. Natural Bioscaffolds

Manufacturing of natural bioscaffolds for current DTE is based on either: a) ECM-derived scaffold construction; b) cell-derived graft generation; or c) autologous in vivo biosheet creation. Collagen-based scaffolds are of major interest in bioengineering as collagenous connective tissue can generate multiple cell types and tissues derived from all three embryonic germ layers.^[12]

Collagen as a main ECM component affects cell migration and attachment and promotes structural ingrowth and

remodeling.^[40,48,49] Processed collagen is utilized in forms of hydrogels^[53] or as scaffold, either as suspended base material^[21,27,50] combined with reinforcing meshes^[54] or as component of a hybrid-scaffold.^[3,50] However, matrices made from purified forms of collagen often fail to maintain integrity when applied in clinical settings (e.g., wound dressing, hernia repair).^[40,51] Only recently, the first skeletal-muscle-derived dECM hydrogel, built in a “collagen-based self-assembly process” supplemented by natural genipin-crosslinking, was introduced for DTE by Boso et al.^[36] The acellular porous composite exhibited minimized enzymatic degradation, increased viscosity, and optimized biomechanical stability compared to non-crosslinked scaffolds. In vitro biocompatibility studies by co-seeding of human dermal fibroblasts and human skeletal muscle cells affirmed active cell proliferation and myogenic regeneration on these dECM scaffolds.^[36] Radial myofiber alignment within the diaphragm can be emulated by processing fibrillar type I collagen with a freezing liquid nitrogen technique.^[27] When the collagen suspension is poured into a mold in a central stainless-steel freezing tube setup, it freezes from the center outwards creating the desired radial fiber alignment. Stainless-steel affects the collagen to create pore sizes of 70–100 μm , which could be suitable for muscle cell ingrowth in the diaphragm as resident myofibers measure 8–109 μm in diameter.^[27] A dual layered collagenous composite consisting of a radially aligned porous collagen layer reinforced by a layer of compressed collagen confirmed that radial pore alignment facilitated deeper ingrowth into the graft and provided for satisfactory integration into the surrounding tissue.^[47] In a leporine model, diaphragms supplied with radial pore oriented collagen scaffold composites (RP-Composites) exhibited similar compliance and pressure resistance compared to NDs, as opposed to GTX.^[46] Moreover, all SIS failed with a 100% reherniation rate in comparison to 22 % in RP-Composite and 17 % GTX recipients.^[46] Overall, the absorbable biocomposite induced significantly lower foreign body giant cell reaction and increased collagen deposition, though a slight tendency for calcification as against the conventional synthetic mesh was notable. Surprisingly, the two scaffold types did not differ with regards to reherniations rates, even though RP-Composites reestablished native diaphragmatic compliance more closely.^[46] An additional comparative study not included in our initial search contrasted the clinical gold standard GTX, the most commonly employed non-crosslinked acellular collagen matrix (ACM) SIS and a highly cross-linked novel ACM (Matricel). Matricel was associated with pronounced adhesion formation and reduced compliance in comparison to NDs, and its use to treat diaphragmatic defects was discouraged.^[52]

Combining several layers of materials with different properties for augmentation of in vivo stability is realized through mesh reinforcement or multilayer assembly in the sense of a “sandwich technique”.^[9] Vicryl-mesh reinforced collagen composites, which have been characterized previously,^[21] failed to maintain tensile strength which was reflected in bulging at implantation

Figure 3. Evaluation of Risk of Bias using SYRCLÉ's risk of bias tool. Studies were assessed for 10 bias parameters and categorized according to not fulfilled (x), fulfilled (✓), not available (n/a) and unclear (?). Three groups (Arai et al. 2020, Boso et al. 2021 and Shieh et al. 2017) did not use animals in their studies, so the assessment parameters 'random animal housing' and 'animal assessment for outcome' could not be answered. Another three papers (Gubareva et al. 2018, Gubareva et al. 2019 and Sotnichenko et al. 2018) were assessed n/a in all columns because they did not compare two intervention groups, thus the SYRCLÉ's risk of bias tool could not be applied.

Table 2. Decellularization methods employed in the last ten years.

Group	Piccoli et al.	Fallas et al.	Trevisan et al.	Gubareva et al.	Davari et al.	Liao et al.	Sesli et al.	Boso et al.
Animal model	Murine (mouse)	Murine (mouse)	Murine (mouse)	Murine (rat)	Human	Murine (rat)	Murine (rat)	Porcine
Organ	Diaphragmatic muscle	Diaphragmatic muscle	Diaphragmatic muscle	Diaphragmatic muscle	En bloc left hemi-diaphragm	Hemidiaphragm	Entire diaphragm	Muscles (SKM; not specified)
Method	n/a	n/a	n/a	Bioreactor-based standard agitation method + retrograde perfusion	n/a	Continuous agitation on orbital shaker	Not given	Incubation ± continuous agitation (for some steps)
Prior treatment	Washed 1x in PBS and conserved in PBS-P/S	Washed in PBS (with whole rib cage)	Washed 2x in PBS	Cannulation with 22 G intravenous catheter; flushed with sterile PBS; perfusion rate 6 mL min ⁻¹	PBS containing 1% penicillin, 1% streptomycin, 1% amphotericin B	Washed 1x in PBS	Washed 1x in PBS; stored in PBS-P/S at 4 °C until decellularization	Disinfection with betadine 10%, several washes with sterile PBS
Decell steps	t	t	t	t	t	t	t	t
1	Deionized water (4 °C)	Deionized water (Ad) (4 °C)	Deionized water (Ad) (4 °C)	4% SDC (RT)	24 h	4% SDC (RT)	24 h	0.5% SDS
2	4% SDC (RT)	4 h	4% SDC (RT)	4 h	4% SDC (RT)	4 h	4% SDC (RT)	24 h
3	2000 kU DNase-I in 1 M NaCl (RT)	2000 kU DNase-I in 1 M NaCl (RT)	2000 kU DNase-I in 1 M NaCl; (RT)	2000 kU DNase-I (in calcium and magnesium; RT)	2000 kU DNase-I (RT)	2000 kU DNase-I (RT)	1% SDS	24 h
4	“Washing in water”	Washed in water	Washed in water	2 mM EDTA in MilliQ water (RT)	2 mM EDTA in MilliQ water (RT)	2 mM EDTA in MilliQ water (RT)	Washed in PBS	Washed in PBS
5	Washed in deionized water	Washed in MilliQ water	Washed in deionized water	2 mM EDTA in MilliQ water (RT)	2 mM EDTA in MilliQ water (RT)	2 mM EDTA in MilliQ water (RT)	Triton X-100	1 h
Cycle duration	31 h	31 h	31 h	5.2 h	58 h	48 h	73 h	31 h
Cycles	1 to 4	3	3	1	25	1	1	4
Post cycle rinse	Washed in deionized water	Washed in MilliQ water	Washed in deionized water	PBS	PBS	PBS (sterile)	PBS	Deionized water
Complete duration	Approximately 4 to 8 d	Approximately 196 h	Approximately 103 h	≤1 day	Approximately 1400 h	72 h	Approximately 73 h	Approximately 196 h (124 h + 72 h incubation)

site.^[53] This can be traced back to the fact that Vicryl only retains a fifth of its initial tensile strength two weeks post-implantation (as reported by the supplier), even though it should withstand degradation until 60 to 90 days in vivo.^[53] Beyond mesh reinforcement, a widely studied approach proposes a tri-layer scaffold combining two layers of ingrowth-promoting, elastic material with high tensile strength (e.g., ECM scaffolds) which enclose a layer of cell delivery vehicle (e.g., a collagen-based hydrogel).^[8,54–56] However, multilayering bears the risk of loss of strength due to delamination, which represents a major limitation in multi-layered dECM scaffolds like Surgisis.^[39]

Regarding cell-derived composites, a novel tissue-engineered approach for diaphragmatic repair established a solely cell-based tubular construct from multicellular spheroids (MCS). Bearing in mind the potential side effects of foreign prosthetic scaffolds on the host tissue, such as granulation, allergic reaction and infection, Zhang et al. created initially scaffold-free grafts.^[57] Normal human dermal fibroblasts (NHDFs) and human umbilical vein endothelial cells (HUVECs) were arranged via 3D-printing on a needle-array and further processed to create flat cellular patches. These cell-based fibroblast sheets integrated adequately during growth and allowed for regeneration of striated muscle fibers and neuronal networks whilst stimulating neovascularization in the rat model. No reherniations, rib cage deformities, or postoperative adhesions were observed until 710 days after transplantation, whereas control Vicryl scaffolds performed poorly with a 17 % survival and—within that—100 % herniation rate at 7 weeks post-implantation.^[57]

Apart from in vitro fabrication, an in vivo preparation method was recently introduced by Suzuki et al., showing that the generation of autologous collagen connective tissue can be induced by subcutaneous embedding of silicon plates which function as a biosheet mold. After 4 weeks, the biosheets are extracted and used as sheet-type collagenous scaffold patches, which makes clinical application in cases of recurring diaphragmatic hernia and—through maturation in a parent—in neonatal CDH care conceivable.^[12] Unlike GTX Soft tissue Patches and Seamdura, the tissue-engineered two-ply biosheets exhibited low herniation rates and showed signs of diaphragmatic muscle regeneration.^[12]

2.6. Synthetic Biocomposites

The clinical standard prosthesis in diaphragmatic repair is the synthetic non-degradable biomaterial ePTFE (GTX).^[58] Novel scaffolds made of biopolymers such as polylactic acid (PLA)^[22] and polycaprolactone (PCL)^[3] are employed in TE for their biodegradable nature, which makes them attractive for soft tissue repair, for example, wound healing.^[40] Nanofibrous scaffolds can be constructed via electrospinning technique which manufactures biodegradable polymers upon requested 3D structure, and biomechanical, physical and chemical properties.^[22] Only recently has electrospun PLA been assessed and affirmed for its support of cellular adherence and proliferation in a subcutaneous immunocompetent rat implantation model, with application in diaphragmatic hernia repair as a future objective.^[22] In a murine orthotopic repair model, aligned electrospun PCL/collagen type I hybrid scaffolds exhibited highly elastic behavior, allowed for early muscle fiber ingrowth and myotube formation, and pos-

sessed mechanical properties similar to the ND at 2, 4, and 6 months after implantation.^[3]

2.7. Ameliorating Tissue Function through Processing and Bioactive Additives

Diverse techniques have been tested in attempt to improve in vivo performance of bioscaffolds, including the incorporation of materials such as glycosaminoglycans and amino acids, different nanostructures like carbon nanotubes, hydroxyapatite nanocrystals, and zirconium oxide nanoparticles, as well as physical, chemical, and enzymatic crosslinking methods.^[36,40] The degree of crosslinking influences the balance between resistance to degradation and allowance for cellular infiltration. Chemical crosslinking is a delicate matter as evoked cytotoxicity and denaturation may impair scaffold functionality.^[59] To address the difficulties of adverse cytotoxic effects, natural crosslinkers such as genipin are employed.^[36,60] Overall practicability of currently available physical crosslinking methods remains unsatisfactory.^[59]

Non-functionalized crosslinking primarily enhances scaffold stability. Crosslinked random porous type I collagen scaffolds chemically crosslinked with 1-ethyl-3-(3-dimethylaminopropyl)carbodiimide (EDC) and N-hydroxysuccinimide (NHS) showed no evidence of reherniations on a macroscopic level when implanted in murine diaphragmatic defects. On the microscopic level, slow scaffold degradation, muscle cell ingrowth, and deposition of ECM proteins and mesothelial cells were observed at transplantation site.^[21]

Upon mounting of bioactive components, which translates to functionalized crosslinking, unique characteristics of the supplemented agent are added.^[61] One main target of functionalized crosslinking in DTE is vascularization. Blood vessel growth is a complex process finely coordinated by ECM components, resident endothelial cells, stimulatory molecules, and growth factors. Guided vascularization may either be achieved by stimulation of the native ECM or incorporation of allogenic ECM, with or without the addition of angiogenic agents, such as hepatocyte growth factor (HGF), VEGF, and stromal cell-derived factor 1 α (SDF-1 α).^[31] Crosslinking the polysaccharide heparin stimulates myogenic or vascular regeneration at the implantation site as heparin is capable of sequestering and binding growth factors such as HGF and VEGF.^[28] Prior studies assessed the influence of VEGF added to porous silica gels with or without myoblasts, which applied on acellular diaphragmatic matrices increased vascularity yet at the expense of aggravated inflammation, fibrosis, and contraction.^[28,62] A current study observed heparin to accelerate early angiogenesis in collagen scaffolds, however a post-operative levelling off phenomenon was visible after 12 weeks with adjusted levels to those of comparison groups that received VEGF- and HGF-functionalization.^[28] Long-term vascularization across all groups was not improved significantly.^[28] Another desirable feature alludes to boosting tissue regeneration by addition of growth factors, such as insulin-like growth factor 1 (IGF-1). Unexpectedly, adding IGF-1 as a highly mitogenic factor with eminent muscle regenerative potential to Vicryl collagen scaffolds did not reinforce muscle ingrowth from the ND.^[53,63] Although morphological integration was given, eventrations oc-

curred in all cases, indicating poor scaffold resistance and rapid degradation.^[53]

A preclinical functionalization approach not delivered by our search investigated advancements of GTX. Preliminary findings of this in vitro study reported possible enhancement of tissue integration by coating with a combination of polydopamine and platelet-rich fibrin (currently used in oral or maxillofacial surgery for its tissue regenerative capacity).^[58]

2.8. Recellularization

Full and functional coalescence with the ND is based on cellular recolonization of the implanted graft, which is either initiated prior to implantation in a laboratory setup or induced within the host organism. Recolonization of both de novo generated and dECM-based grafts has advantageous effects on their integrative and regenerative capacity. For instance, while sole decellularization may negatively impact the tissues' in vitro biomechanical properties, recellularization can further recover essential microcirculation and functional contractile properties in the host.^[11] Graft recellularization is generally based on three core concepts: 1) in vitro cell seeding; 2) in vitro retrograde perfusion of pre-existing vascular structures; and 3) direct cell injection into the targeted structure in vitro or in vivo. In DTE, cellular application is only obtained by scaffold repopulation via direct seeding of cells through various techniques, including 3D printing, growth-factor induced colonization, pressurized cell infusion systems, and specific bioreactors.^[9,11,22,37,42,54] Ideal cell populations for restoration of native tissue function should demonstrate high-grade proliferation, differentiation, and self-regeneration capability.^[38,42] On that basis, stem cells are the preferred cell type ranging from induced pluripotent stem cells, mesenchymal stromal cells (MSCs) to adult muscle stem cells. Mesenchymal stromal cells derived from amniotic fluid (AF-MSCs),^[9,22,53] adipose tissue (AdMSCs),^[39] and bone marrow (BM-MSCs)^[11] are comprehensively investigated for diaphragmatic tissue repopulation. MSCs create an anti-inflammatory, pro-angiogenic environment and prevent exuberant inflammatory reactions through three major action modes: a) the expression of interleukin-1 receptor antagonist; b) secretion of anti-inflammatory cytokines which downregulate macrophage response; and c) regulation of macrophage switch from a pro-inflammatory M1-state to a more regulatory or anti-inflammatory M2-state.^[22,64] What is more, MSCs induce extracellular matrix deposition by resident cells and their proliferation, differentiation, and repopulation upon the newly synthesized structures.^[22] The use of AF-MSCs is mainly intended for application in congenital diaphragmatic defects, as extracting these undifferentiated cells from an autologous source via amniocentesis offers the advantage of minimal immune response and secured disposability.^[9,22,54,55,65] Cells can be harvested, processed, and prepared for implantation precisely timed from prenatal diagnosis of the congenital diaphragmatic defect to calculated date of birth. Alternatively, BM-MSCs constitute an inherently available cell type with known immunomodulatory effects.^[11,66] Application of more lineage-committed cell types is another viable option for muscle regeneration, for instance by the use of human muscle progenitor cells (hMPCs).^[42]

A broad overview on recellularization TE methods for diaphragmatic repair can be found in **Table 3**.

Many factors ought to be considered for repopulation of acellular scaffolds. One study found scaffold type, seeding density, and time in 3D culture to interact in a significant manner. In the corresponding study, under almost all seeding conditions, a human-derived hydrogel (Vitrocol) provided superior cell viabilities for the culture of AF-MSCs compared to a bovine-derived collagen sheet (SurgiMend).^[54] Another approach endorsed electrospun PLA to be a suitable scaffold material for short-term culture of AF-MSCs, as it supported cell adherence and proliferation.^[22] In vivo host inflammatory responses observed in heterotopically implanted unseeded and seeded PLA scaffolds differed in cell composition and remodeling processes. In contrast to unseeded grafts, AF-MSCs seeded scaffolds presented reduced levels of eosinophils, increased matrix degradation and collagen fiber deposition.^[22] In a recent murine study by *Liao et al.*, AF-MSCs were seeded onto decellularized matrices using an infusion system based on pressurized perfusion of a cellular suspension through the fixated scaffold.^[9] The generated AF-MSCs composites displayed enhanced regenerative capacities for diaphragmatic skeletal muscle repair as opposed to dECM alone, through vascularization and functional recovery of muscular, neuronal, and tendinous structures 4 months after implantation. No hernia recurrence or clinical signs of weakness could be detected.^[9] Apart from AF-MSCs colonized grafts, the first pre-clinical approach to transplant a dECM scaffold reseeded with allogeneic rat BM-MSCs in murine diaphragmatic defects was likewise successful in reestablishing a native diaphragmatic biomechanical function.^[11]

A more lineage-committed recellularization approach with human muscle progenitor cells (hMPCs) seeded onto a dECM scaffold examined the progenitor cells to grow into and repopulate all layers of the dECM scaffold that further regained functionality (confirmed by metabolic active myotubes inside the dECM) in a murine model.^[42] As a sign of stem cell niche preservation, the scaffold was able to respond to damage with constructive remodeling. A cytotoxicity assessment detected characteristic indicators of stem cell niche reconstitution such as: a) an increase in the PAX7⁺ cell population; b) progressive satellite cell carried remodeling with fibronectin production; and c) increased gene expression of LAMA1.^[10,42]

3. Discussion

3.1. Novel Tissue-Engineered Grafts Outperform Conventional Grafts

Altogether, dECM matrices restore, maintain, and improve in vivo diaphragmatic tissue function by advancing constructive remodeling and inducing myogenic, vascular, and neuronal regeneration in small animal models.^[11,31] dECM scaffolds: 1) induce less severe immunological response with little to no encapsulation compared to conventional patches;^[10] 2) have a pro-angiogenic influence and promote in situ vascularization;^[10,11,31] 3) encourage efficient local muscle regeneration;^[9-11,31,43,44] 4) promote neuronal integration;^[10,11,43] 5) improve post-operative outcomes with lower reherniation rates;^[9,10,24,43] and 6) restore diaphragmatic function.^[9-11,31,41,42] Decellularization-based scaffold

Table 3. Studies investigating recellularization and cell-based construction methods for diaphragmatic repair.

Study group	Gubareva et al.	Zhang et al.	Lesage et al.	Liao et al.	Shieh et al.	Sesli et al.	Trevisan et al.	Arai et al.
Study	Orthotopic Transplantation of a Tissue Engineered Diaphragm in Rats	Regeneration of Diaphragm with Bio-3D Cellular Patch	Modulation of the Early Host Response to Electrospun Poly(lactic Acid) Matrices by Mesenchymal Stem Cells from the Amniotic Fluid	Tissue Engineering to Repair Diaphragmatic Defect in Rat Model	Comparisons of Human Amniotic Mesenchymal Stem Cell Viability in FDA-Approved Collagen-Based Scaffolds: Implications for Engineered Diaphragmatic Replacement	Decellularization of Rat Adipose Tissue, Diaphragm, and Heart: A Comparison of Two Decellularization Methods	Generation of a Functioning and Self-Renewing Diaphragmatic Muscle Construct	Cryopreservation Method for Spheroids and Fabrication of Scaffold-Free Tubular Constructs
Cell type	Rat BM-MSCs	HUVECs (10–30%) and NHDFs (70–90%)	1) hAF-MSCs; 2) Fibroblasts (CTRL)	hAF-MSCs	hAF-MSCs	AdMSC	hMPCs	NHDF
Cell source	Femur/tibiae (flushed with PBS)	Purchased from Lonza	1) Diagnostic amniocentesis at 17 weeks of gestation; 2) foreskin biopsy	Amniocentesis (33-year-old healthy Caucasian female, non-hispanic donor at gestational age 20 weeks)	Amniocentesis samples (20 and 37 weeks of gestation) from fetuses with a normal karyotype	Subcutaneous and gonadal adipose tissues of 2 male albino rats (Wistar; 250–300 g)	Human skeletal muscle biopsies	Purchased from Lonza
Repopulation sample size (grafts) with following implantation	n = 5	n = 5	n = 6 (per implant group (four groups) and time point)	n = 40	None	n = 5	n = 7	n/a

(Continued)

Table 3. (Continued).

Study group	Gubareva et al.	Zhang et al.	Lesage et al.	Liao et al.	Shieh et al.	Sesli et al.	Trevisan et al.	Arai et al.
Animal model for implantation	8 weeks male rats (Lewis; 250 ± 50 g)	8–12 weeks male F344/N-rnu nude rats	3 months immune competent male rats (Wistar)	7 weeks female rats (Sprague Dawley 150–175 g)	None	None	None	None
Implantation site	Orthotopic	Orthotopic	Subcutaneous	Orthotopic	n/a	n/a	n/a	n/a
Passage at use	n/a	5–10	n/a	3	n/a	2	5–6	n/a
Application method	Seeding	Regenova bio-3D printer with Kenzan method	Seeding	In vitro infusion system	Seeding	Seeding	Seeding	Regenova bio-3D printer with Kenzan method
Cell density	50,000 cells/cm ²	Total cell counts of 20,000, 25,000, 30,000	100,000 cells/cm ²	900–1000 cells/cm ²	50 000; 100 000; and 150 000 cells/mL	200,000 cells/mL	500,000 cells per patch	30 000 cells
Scaffold type	Murine diaphragmatic dECM	None (scaffold-free fibroblast sheet)	Electrospun PLA matrices	Murine diaphragmatic dECM	1) Vitro Col; 2) SurgiMend	Murine diaphragm (rat)	Murine (mouse) diaphragmatic dECM	None (scaffold-free fibroblast sheet)
Patch size	Defect size: 1.5 cm × 2.5 cm or 80 % of the left hemi-diaphragm; patch size n/a	12 mm × 10 mm rectangular defect; patch size n/a	1 cm × 1 cm or 2.5 × 2.5 cm	Defect size: 1.2 mm × 1.2 mm circular left diaphragmatic defect; patch 2–3 mm overlap	1) Liquid form on ice; (2) 5 cm × 6 cm	25 mm ²	35 mm ²	n/a

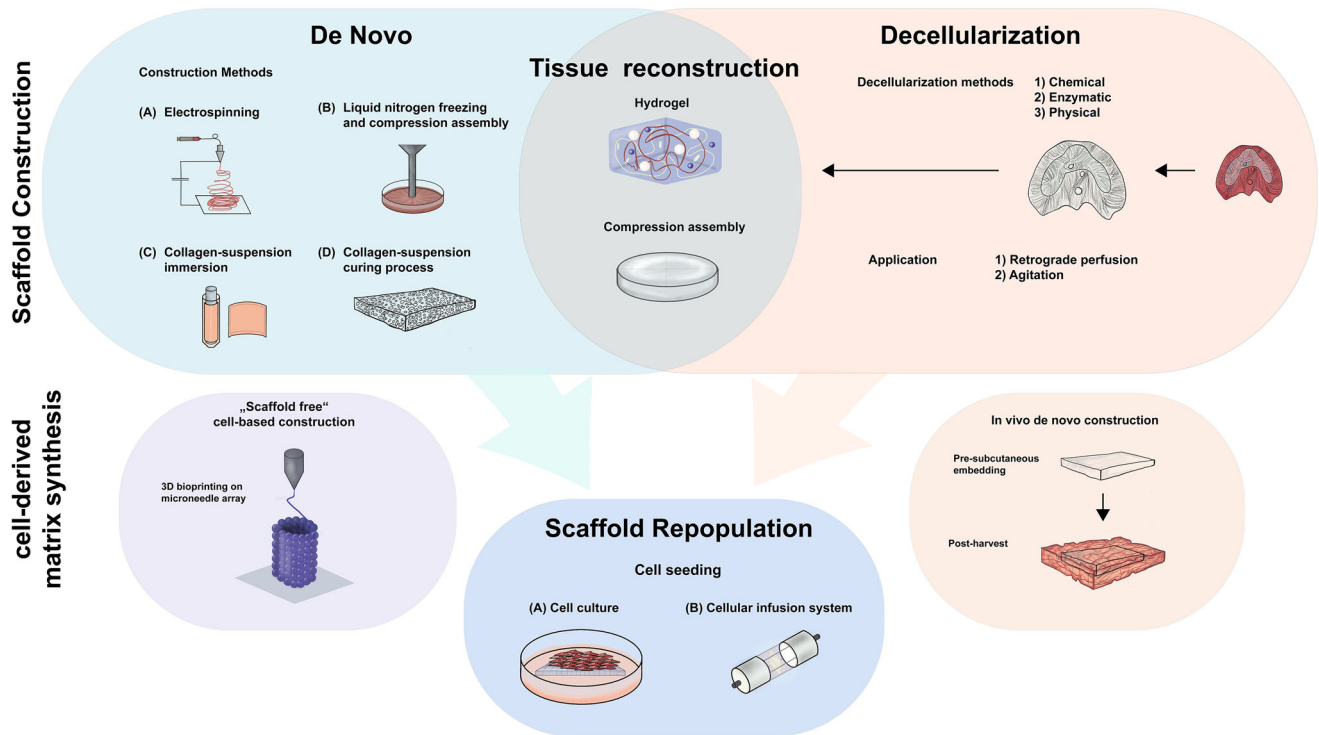


Figure 4. Overview of TE for the diaphragm. The two main pillars of ECM-based scaffold construction are de novo construction and decellularization, whereby these two methods can be combined (tissue reconstruction). For recellularization, cells are seeded onto ECM scaffolds in a conventional cell culture setup or cellular infusion system. Cell-derived matrix synthesis in current DTE is either attained by cellular 3D printing or in the sense of "in vivo de novo construction" as host cells repopulate a subcutaneously implanted scaffold.

folds provide an excellent base material for recellularization and additionally sustain myogenic differentiation on the proteomic level from early on, which is reflected in the reestablishment of organotypic properties instead of scar tissue formation.^[11]

Due to their diverse nature, de novo generated scaffolds exhibit distinct properties in restoring diaphragmatic function. Non-functionalized crosslinking in collagen scaffolds tended to increase biomechanical resilience and resistance to degradation, while ensuring muscular and ECM regeneration.^[21] While RP-Composites exhibited tendencies for enhanced regeneration and mitigated alloresponse, no differences in reherniations rates were observable in comparison with conventional scaffolds in clinical use.^[46] Vicryl reinforced collagen composites demonstrated rapid degradation and limited strength, reflected in high recurrence rates, whilst functionalized crosslinking with IGF-1 had no relevant impact.^[57,53] Functionalization with pro-angiogenic agents resulted in no beneficial long-term effect either.^[28] A novel dECM-based hydrogel outperformed a non-crosslinked scaffold in terms of resistance to degradation and biomechanical stability.^[36] Both cell-based fibroblast sheets^[49] and autologously grafted biosheets^[12] induced muscular regeneration, while vascular and neuronal connectivity was reestablished in fibroblast sheet repair. PCL/collagen hybrid scaffolds likewise showed signs of muscular regeneration and proved to be biomechanically coequal to the ND.^[3] Synthetic PLA was affirmed to be suitable for in vitro cell recolonization.^[22]

Recellularized matrices have the potential to improve biomechanical behavior and interaction with the microenvironment at

graft site.^[11,42] Besides, composite tissues with stem cells have been ascertained to lead to improved functional tissue regeneration and ameliorated healing.^[9,11] Current TDE approaches are illustrated in **Figure 4**. An overview comparing tissue-engineered scaffolds to meshes in current clinical use as their controls, extended by other current patches for CDH treatment, is provided in **Table 4**.

3.2. Intrinsic Challenges: Engineering Around Diaphragmatic Issues

Scientific dissent on fundamental questions about definitional parameters, preferred animal models, and favorable tissue and cell types for DTE shape the experimental scope in this diverse field, generating manifold engineering approaches.

What is considered to be successful skeletal muscle decellularization is defined inconsistently. In general, decellularization refers to the removal of cellular material and quality criteria allude to remnant nuclei content. As skeletal myofibers form a functional syncytium originating from fused progenitor cells—per definition—removal of cellular content would include the elimination of myofiber structures. In a study by *Piccoli et al.*, decellularization was rated successful when dECM were depleted of nuclei content while myofibers were preserved. By contrast, the *Gubareva* study group defined effective decellularization by complete depletion of nuclei content and concurrent myofiber removal.^[11,41] It remains unclear whether the potential advan-

Table 4. Comparison of grafts in current clinical use and implanted tissue-engineered grafts. Exclusively tissue-engineered grafts that employed meshes in current clinical use and certified meshes as their control group were included.

	Category	Product	Composition	Advantages	Disadvantages	Herniation rates
Grafts in current clinical use (CTRL in current animal studies)	Synthetic non-resorbable	Gore-Tex	ePTFE	<ul style="list-style-type: none"> Established clinical application (gold standard in CDH treatment) High thermal, chemical, and mechanical stability and durability Low coefficient of friction 	<ul style="list-style-type: none"> Rigidity Lack of growth-potential and shrinking High hydrophobicity Low biocompatibility, evocation of strong FBR (pronounced M1-response) and encapsulation Limited vascular and muscular ingrowth 	<p>Experimental: 17–45%^[10,12,46]</p> <p>Clinical: 28–50%^[67–69]</p>
Grafts in current clinical use (not compared in current animal studies)	Natural resorbable	Surgisis	Porcine acellular small intestinal submucosa	<ul style="list-style-type: none"> Established clinical application Fast integrative capacity Biomechanical flexibility 	<ul style="list-style-type: none"> Rapid graft degradation Xenogeneic donor tissue 	<p>Experimental: 100%^[46]</p> <p>Clinical: similar to Gore-Tex^[70]</p>
Grafts in current clinical use (not compared in current animal studies)	Composite non-resorbable	Gore-Tex/Marlex	ePTFE and type 1 monofilament microporous polypropylene (Marlex) composite	<ul style="list-style-type: none"> Lower recurrence rates compared to Gore-Tex Minimal adhesion formation 	<ul style="list-style-type: none"> Potential disadvantages of Gore-Tex 	<p>Clinical: 3.6%^[71]</p>
Certified product (not routinely applied in diaphragmatic defects)	Natural resorbable	Alloderm	Acellular non-cross-linked human cadaveric dermis	<ul style="list-style-type: none"> Neovascularization 	<ul style="list-style-type: none"> Lack of tensile strength Allogeneic tissue from diseased donor Xenogeneic donor tissue 	<p>Clinical: 40%^[72]</p>
	Natural resorbable	Permacol	Crosslinked collagen sheet from porcine dermis	<ul style="list-style-type: none"> Minimal inflammatory response Increased resistance to degradation Neovascularization 	<ul style="list-style-type: none"> Rapid in vivo attenuation before any tissue regeneration 	<p>Clinical: 0%^[73]</p> <p>Experimental: 73%^[12]</p>
	Composite resorbable	Seamdura	Artificial dural substitute (copolymer of P(LA/CL) + polyglycolic acid (PGA)	<ul style="list-style-type: none"> Elasticity and tear resistance, strength (PGA reinforcement) (according to supplier) 	<ul style="list-style-type: none"> Lack of growth-potential and tensile strength 	<p>Experimental: 100%^[74]</p>
	Composite resorbable	Vicryl	Knitted or woven mesh from polyglactin 910	<ul style="list-style-type: none"> Temporary support with fast integration 		

(Continued)

Table 4. (Continued).

Category	Product	Composition	Advantages	Disadvantages	Herniation rates
Tissue-engineered grafts	Natural resorbable Acellular dECM Scaffolds	Decellularized diaphragmatic skeletal muscle (e.g., murine)	<ul style="list-style-type: none"> ■ High biocompatibility ■ Substantial integrative capacity (vascular, muscular, neuronal) ■ Highly stable and prolonged angiogenic stimulus^[31] ■ Restoration of diaphragm functionality ■ Higher efficiency of sustaining host tissue regeneration and function recovery 	<ul style="list-style-type: none"> ■ Xenogeneic donor tissue 	Experimental: 0% ^[10]
Natural resorbable	Cellular dECM Scaffolds	Mouse dECM + hMPCs	<ul style="list-style-type: none"> ■ Coequal biomechanical properties (compared to ND) ■ Pro-regenerative capacity (muscular, vascular regeneration) ■ Preservation of functional stem cell pool with positive damage-response ■ Easy storability 	<ul style="list-style-type: none"> ■ Xenogeneic donor tissue 	Experimental: 0% ^[42]
Natural resorbable	Bio-3D cellular patch	Scaffold-free fibroblast sheets from MCS	<ul style="list-style-type: none"> ■ High elasticity and strength ■ Substantial integrative capacity (vascular, muscular, neuronal regeneration) ■ Ethically innocuous allogeneic cell source (NHDFs and HUVECs) ■ 3D printing for specific prerequisites 	<ul style="list-style-type: none"> ■ Complex production 	Experimental: 0% ^[57]
Composite resorbable	RP-Composite	Radial pored orientated collagen scaffold + 4-ply SIS, combination via crosslinking	<ul style="list-style-type: none"> ■ Coequal biomechanical properties (compared to ND) ■ Less pronounced FBR than Gore-Tex 	<ul style="list-style-type: none"> ■ Calcification tendency ■ Encapsulation ■ Xenogeneic donor tissue 	Experimental: 221% ^[46]
Natural resorbable	Biosheets	Autologous collagenous connective tissue membranes	<ul style="list-style-type: none"> ■ Stem cell recruitment ■ Pro-regenerative capacity (muscular regeneration) ■ Similar burst strength and elasticity (compared to ND) ■ Autologous harvest 	<ul style="list-style-type: none"> ■ Muscular regeneration only at borders of implanted graft 	Experimental: 21% ^[12]

tages of myofiber preservation outweigh the possible disadvantages.

As growth restriction is one of the leading causes for patch failure in neonatal defect care, fast-growing and larger animal models like rabbits and lambs are preferred in CDH models, yet many studies rely on murine models, likely for their practicability.

The diaphragm as a musculotendinous organ raises the central question whether full dynamic and functional recovery is ideally attained by reconstruction with a tendinous or muscular tissue-engineered prosthetic, and likewise whether repopulation should be performed with the corresponding progenitor cells. While tendinous or muscular patches could be applied in minor lesions, major disabilities requiring a partial or complete diaphragmatic surrogate potentially call for force-generating skeletal muscle grafts. For diaphragmatic defect closure in CDH animals models, tendinous grafts are preferred as the diaphragm consists of a considerable tendinous portion and native muscle residue in diaphragmatic lesions may compensate for a non-contractile graft.^[8,54,74] Diseases with muscular insufficiency as the underlying pathological mechanism necessitate contractile properties for active movement. In an atrophic murine model, the auspicious outcome of dECM patches ameliorating host diaphragmatic function opens new prospects for construction of diaphragmatic supports or surrogates.^[41]

A definite prerequisite for regeneration and maintenance of muscular grafts is neuronal connectivity with the surrounding tissue, in contrast to tendinous scaffolds.^[8,75,76] The presence of neuronal networks and re-innervation have only been described in murine models.^[10,57] Another integral factor for muscle functionality and proper force transmission is based on muscle fiber continuity, whereas discontinued myofiber architecture presupposes to volumetric muscle loss.^[13,77] To assess functional restoration, an *in silico* finite element model of murine diaphragms approximates maximum contractile force and excursion ability in patch-repaired diaphragms.^[10] In the clinical context, sonographic measurement of diaphragmatic excursion ratio has been identified as a predictor for long-term respiratory outcome, making *in silico* studies an interesting tool for preclinical patch performance assessment.^[78] Bearing in mind the concept of imitating native diaphragmatic architecture and composition, preservation of the heterogenous local muscle structures could be favorable.^[42,79] In a volumetric muscle loss model, the combination of resident adult muscle stem cells (“satellite cells”) with other muscle resident cells (e.g., endothelial cells) on decellularized tissue, showed restoration of muscle function as opposed to single-cell-type grafts.^[79] Combined cellular application has only been realized in cell-derived scaffold construction with NHDFs and HUVECs, but not in recellularization of dECM diaphragmatic patches.^[57]

Reduction of patch repair associated morbidities is feasible if challenges originating from inherent scaffold properties and their interaction with the implantation environment are understood. Augmentation of *in vivo* performance depends on the scaffold's ability to integrate ideally into the host tissue, for which sufficient vascularization is crucial. Vascular insufficiency may result in hypoxia and nutrient deficits leading to the formation of fibrotic areas and necrotic cores, hence increasing the risk of mechanical and immunogenic graft failure.^[31] One attempt to improve blood supply at implantation site is to attach the

highly vascularized omentum to the scaffold. However, applying this technique in Vicryl collagen scaffold repair was a likely contributor to more rapid scaffold degradation.^[27] An advantage of dECM scaffolds may be their maintenance of bioactive molecules such as growth factors, whereby Omics — which are yet to be done for the diaphragmatic muscle and derived dECM scaffolds — could provide essential insights on the tissue's regenerative properties. Even though the finding that dECM scaffolds are non-immunogenic leaves systemic immunosuppression redundant, deliberate regulation of the host response by induction of a M1 to M2 macrophage shift could create a pro-regenerative inflammatory state conducive for efficient integration into, and dynamic restoration of the native tissue.^[11,30] Heterotopic subcutaneous implantation of dECM-grafts can serve as an assessment method for host immune response, allowing scaffold sensitivity testing for high risk of rejection without the need for necropsy after orthotopic implantation for histological evaluation. However, it must not be neglected that the immune reaction to heterotopic and orthotopic transplantation (OTX) may differ to some extent.^[11,35]

Besides patch properties, *in vivo* performance of tissue-engineered constructs depends on multiple characteristics of the diaphragmatic defect itself. Complications of thereupon required patch repair occur in varying degrees according to pivotal variables — the 4 “S”: implant site, affected side, defect size, and integration speed.

1) Implantation site: Scaffold position as a crucial determinant for muscle ingrowth cannot be ensured when the scaffold is implanted into the diaphragmatic central tendon, resulting in absent ingrowth from the tendinous side.^[21,47]

2) Affected side: Adhesions most frequently occur on the abdominal diaphragmatic side facing the liver,^[3,11,21,28,43] while eventrations and reherniations are often observed in the left hemi-diaphragm,^[48,49] although liver herniations are reported in patch repair as well.^[10,12,47] Clinical data reports similar morbidity rates in right- and left-sided CDH, yet higher postoperative mortality rates in patch-repaired right-sided diaphragmatic CDH.^[80] For realistic assessment of relevant complications, a right-sided hemi-diaphragmatic defect model may be favorable.

3) Defect size: Defect size represents a decisive factor, as biomechanical force distribution along the scaffold surface and sufficient blood supply influence long-term *in vivo* scaffold performance in extensive impairments.^[8,21] In clinical CDH treatment, defect size is one of the main relevant neonatal predictive outcome parameters, along with positional factors in accordance with (2) (e.g., liver herniation, stomach position).^[13,23,81]

4) Integration speed: Non-growing synthetic meshes or slowly adapting scaffolds may hamper integral growth within the host organism, and with increasing disproportion lead to the “tethering effect.”^[23] Gauging an equilibrium between scaffold degradation and maintenance of integrity is essential for dynamic endurance and functionality.

3.3. Extrinsic Challenges: Tackling the Transferability Concern and Clinical Implementation

Bridging the gap between experimental research and clinical application constitutes a considerable TE quest which ought to be

addressed for larger-scale implementation. Main extrinsic challenges refer to: 1) on-demand availability, which depends on fast and efficient producibility as well as easy storability; 2) ethical innocuity; and 3) simple surgical handling. As the impairments vary in their urgency to be treated, realistically implementable TE options are limited to on-demand availability. For example, while prenatally diagnosed diaphragmatic diseases come with a certain time frame until birth, some diaphragmatic injuries require immediate defect repair which is best supplied with a readily retrievable prosthetic. De novo generated scaffolds including an adaptable and potentially 3D-printable dECM-derived hydrogel deliver on this promise, yet further studies on applicability as “stand-alone patch” in larger diaphragmatic defects are indispensable.^[36] Furthermore, cost-effective storage conditions should be realized for long-term clinical usability. One study confirmed the best storage conditions for dECM scaffolds to be 2 weeks at 4 °C for fast use or 2 months in liquid nitrogen for longer storage.^[42] Cryo-conservation as found a proper method for storing multi-spheroids.^[82] For cell-seeded composites, best suitable culture conditions with relevant parameters like oxygen tension, mechanical stimuli and dynamic cultures are yet to be determined. Considerations for efficient producibility like cell source, time of harvest, and culture are extended by the aspect of ethical compliance. For feasibility of larger-scale implementation, one must consider that cells and tissues are to be provided in sufficient amounts and from ethically innocuous sources, currently led by autologous sources as both cell (e.g., AF-MSCs) and scaffold source (e.g., biosheets).^[12,22,57]

Beyond engineering a suitable graft, there is no clear consensus in the clinical field in securing its *in vivo* functionality through effective surgical modality. Tissue protective, fast, and minimally traumatic surgery facilitates preservation of the mesothelial lining, which naturally prevents adhesion formation.^[47] Thoracoscopic patch repair as a minimally invasive surgical approach affects lower post-operative morbidity and mortality, but comes at the cost of higher recurrence rates.^[83,84] Moreover, tension-reduced defect closure should be achieved; nonetheless no standardized tolerable tension threshold has been defined yet.^[13] Retrospective data comparing tension-free dome-shaped GTX patches and PR with similar recurrence rates (5.4 % GTX versus 4 % PR) indicates that they might be traced back to extrinsic technical hardships rather than intrinsic patch characteristics.^[85] Retrospective studies report ambiguous data on whether dome-shaped or flat prosthetics should be preferred.^[86,87]

4. Future Outlook

Concerning TE methodology, although there's a myriad of studies dedicated to finding the best DET protocol, there is no data on comparisons of different DET modalities within diaphragmatic TE.^[29,88–90] While DET constitutes the most established decellularization method for the diaphragmatic muscle, future approaches could employ apoptosis-based concepts,^[86] vacuum-assisted decellularization,^[87–89] or other agents, like latrunculin B, which was recently reported to achieve the most efficient skeletal muscle decellularization when contrasted with other DET.^[89,91] Functional comparison of *in vivo* performance of differently decellularized or de novo generated biocomposites is

yet to be performed. To our knowledge, there are no studies contrasting decellularized tendinous to muscular grafts for the diaphragm. A point of future investigations for recellularization could focus on preserving the heterogeneity of native diaphragmatic composition and comparing different recellularization methods in DTE.^[92,93]

In substance defect repair, while there is no methodological DTE standard, all novel tissue-engineered grafts tended to be superior in general outcomes compared to patches in current clinical use. Based on the imposing advantages of some of these novel scaffolds, the next step would entail translation from animal studies to phase-I-studies. TE research for treatment of diaphragmatic muscular insufficiency has not gained much traction yet. Though no curative therapy, one study reported an individual tissue-engineered graft to provide diaphragmatic support and ameliorate residual atrophic muscle function, which opens an innovative area of application.^[41]

In times of organ shortage, creating a tissue composite that closely resembles or even enhances native diaphragmatic function poses a substantial milestone in regenerative medicine. Common shortcomings in transplant medicine, like donor organ scarcity, life-long immunosuppression, and ethical and organizational hardships could be evaded by utilizing an on-demand, non-immunogenic, biologically coequal, and ethically responsible tissue-engineered surrogate.

5. Conclusion

To our knowledge, this is the first systematic review to provide a broad overview on the current state of the art in TE for diaphragmatic applications. The aim of this review is to gather research from the last decade focused on creating an optimal bioscaffold for diaphragmatic repair. Decellularized matrices and de novo constructed biocomposites largely exhibited enhanced behavior in terms of evoked alloresponse, tissue regeneration, and long-term outcome in comparison to prostheses in current clinical use, whereby recellularization even improved their properties. In the light of these findings, translational studies should be envisaged to establish a new clinical standard.

6. Experimental Section

The systematic research on the Medline library was performed via Boolean search on Pubmed and according to PRISMA-P Guidelines.^[94] Inclusion criteria comprised the following items:

- 1) The study is available in full text.
- 2) The published article is available in English.
- 3) Reflecting the current state of the art in diaphragmatic tissue engineering (DTE), the study is not older than 10 years.
- 4) Only original articles are included.
- 5) The study makes TE for the diaphragm subject of discussion.

The authors included *in vivo*, *in vitro* and *in silico* studies of any animal (e.g., canine, murine, porcine models) or human tissue dealing with conventional TE approaches and assessment methods. Animal models with healthy animals and/or autologous control within the same individual were eligible, whereby controls were suitable if untreated or treated with a different intervention.

Publications were excluded if they met one of the following criteria:

- 1) The publication was published over 10 years ago and/or does not reflect the current state of the art of the described model.
- 2) The article is a review, meta-analysis, lecture speech or clinical trial.
- 3) There is no English version of the article available.
- 4) The article treats any other than TE and/or diaphragmatic modification related topics.
- 5) The TE approach is not intended for diaphragmatic repair or augmentation.
- 6) The study compares two or more TE methods in different animal models.
- 7) The article does not report any relevant outcomes for DTE.

The Boolean Search was carried out using the following search term: (decell*[tw] OR recell*[tw] OR tissue engineering [MeSH Terms] OR Tissue scaffold [MeSH Terms]) AND "Diaphragm"[Mesh]. Aiming at providing a wider view, the authors included a free word search for "diaphragm*", thus the alternative search command was: (decell*[tw] OR recell*[tw] OR tissue engineering [MeSH Terms] OR Tissue scaffold [MeSH Terms]) AND ("Diaphragm"[Mesh] OR "diaphragm*" [tw]).

Two independent reviewers conducted data extraction from text, graphs, and attachments of selected studies. In case of missing data, authors were contacted to provide missing information. In case of discrepancies (e.g., relevance of extracted data), a consensual agreement was sought and/or a third independent party was consulted. Risk of bias was evaluated for controlled studies with separate treatment arms; for any other study design risk of bias was not assessed. For animal studies, risk of bias was estimated using SYRCLE's risk of bias tool adapted for animal studies.^[9] For in vitro studies, questions 4) "Were the animals randomly housed during the experiment?" and 6) "Were animals selected at random for outcome assessment?" were excluded. Two independent researchers conducted the quality assessment. Again, in case of discrepancies, a consensual agreement was sought and/or a third independent party was consulted.

Acknowledgements

A.K.B. and K.H.H. contributed equally to this work. The authors thank the scientific community for their research and interest in diaphragmatic tissue engineering. K.H.H. and T.D. are participants in the BIH Charité Clinician Scientist Program funded by the Charité – Universitätsmedizin Berlin and the Berlin Institute of Health. F.K. is a participant in the BIH Charité Advanced Clinician Scientist Program funded by the Charité – Universitätsmedizin Berlin and the Berlin Institute of Health.

Open access funding enabled and organized by Projekt DEAL.

Conflict of Interest

The authors declare no conflict of interest.

Keywords

congenital diaphragmatic hernia, *de novo* scaffold construction, decellularization, diaphragm, muscular dystrophy, recellularization, tissue engineering

Received: December 18, 2021

Revised: March 9, 2022

Published online: April 30, 2022

- [1] B. Bordoni, E. Zanier, *J. Multidiscip. Healthcare* **2013**, 6, 281.
- [2] J. Kocjan, M. Adamek, B. Gzik-Zroska, D. Czyzewski, M. Rydel, *Adv. Respir. Med.* **2017**, 85, 224.

- [3] W. Zhao, Y. M. Ju, G. Christ, A. Atala, J. J. Yoo, S. J. Lee, *Biomaterials* **2013**, 34, 8235.
- [4] P. De Coppi, J. Deprest, *Semin. Pediatr. Surg.* **2017**, 26, 171.
- [5] M. D. Politis, E. Bermejo-Sanchez, M. A. Canfield, P. Contiero, J. D. Cragan, S. Dastgiri, H. E. K. de Walle, M. L. Feldkamp, A. Nance, B. Groisman, M. Gatt, A. Benavides-Lara, P. Hurtado-Villa, K. Kallen, D. Landau, N. Lelong, J. Lopez-Camelo, L. Martinez, M. Morgan, O. M. Mutchinick, A. Pierini, A. Rissmann, A. Sipek, E. Szabova, W. Wertelecki, I. Zarante, M. K. Bakker, V. Kancherla, P. Mastroiacovo, W. N. Nembhard, *Ann. Epidemiol.* **2021**, 56, 61.
- [6] W. E. Reyna, R. Pichika, D. Ludvig, E. J. Perreault, *J. Biomech.* **2020**, 110, 109961.
- [7] M. Dres, A. Demoule, *Curr. Opin. Crit. Care* **2020**, 26, 18.
- [8] D. O. Fauza, *Semin. Pediatr. Surg.* **2014**, 23, 135.
- [9] G. P. Liao, Y. Choi, K. Vojnits, H. Xue, K. Aroom, F. Meng, H. Y. Pan, R. A. Hetz, C. J. Corkins, T. G. Hughes, F. Triolo, A. Johnson, K. J. Moise Jr., K. P. Lally, C. S. Cox Jr., Y. Li, *Stem Cells Int.* **2017**, 2017, 1764523.
- [10] C. Trevisan, E. Maghin, A. Dedja, P. Caccin, N. de Cesare, C. Franzin, D. Boso, P. Pesce, F. Caicci, F. Boldrin, L. Urbani, P. De Coppi, M. Pozzobon, P. Pavan, M. Piccoli, *Acta Biomater.* **2019**, 89, 115.
- [11] E. A. Gubareva, S. Sjoqvist, I. V. Gilevich, A. S. Sotnichenko, E. V. Kuevda, M. L. Lim, N. Feliu, G. Lemon, K. A. Danilenko, R. Z. Nakokhov, I. S. Gumenyuk, T. E. Grigoriev, S. V. Krashenninnikov, A. G. Pokhotko, A. A. Basov, S. S. Dzhimak, Y. Gustafsson, G. Bautista, A. Beltran Rodriguez, V. M. Pokrovsky, P. Jungebluth, S. N. Chvalun, M. J. Holterman, D. A. Taylor, P. Macchiarini, *Biomaterials* **2016**, 77, 320.
- [12] K. Suzuki, M. Komura, K. Terawaki, T. Kodaka, T. Gohara, H. Komura, Y. Nakayama, *J. Pediatr. Surg.* **2018**, 53, 330.
- [13] A. K. Saxena, *Pediatr. Surg. Int.* **2018**, 34, 475.
- [14] S. Costerus, K. Zahn, K. van de Ven, J. Vlot, L. Wessel, R. Wijnen, *Surg. Endosc.* **2016**, 30, 2818.
- [15] A. C. Gasior, S. D. St Peter, *Pediatr. Surg. Int.* **2012**, 28, 327.
- [16] C. Barroso, J. Correia-Pinto, *Eur. J. Pediatr. Surg.* **2018**, 28, 141.
- [17] F. Camela, M. Gallucci, G. Ricci, *Paediatr. Respir. Rev.* **2019**, 31, 35.
- [18] C. F. Bell, S. K. Kurosky, S. D. Candrilli, *Hosp. Pract.* **2015**, 43, 180.
- [19] J. R. Bach, J. Tran, S. Durante, *Am. J. Phys. Med. Rehabil.* **2015**, 94, 474.
- [20] G. Crescimanno, F. Greco, R. D'Alia, L. Messina, O. Marrone, *Neuromuscular Disord.* **2019**, 29, 569.
- [21] K. M. Brouwer, W. F. Daamen, D. Reijnen, R. H. Versteegen, G. Lammers, T. G. Hafmans, R. G. Wismans, T. H. van Kuppevelt, R. M. Wijnen, *J. Tissue Eng. Regener. Med.* **2013**, 7, 552.
- [22] F. Lesage, S. Roman, S. Pranpanus, S. Ospitalieri, S. Zia, J. Jimenez, S. MacNeil, J. Toelen, J. Deprest, *Eur. J. Pediatr. Surg.* **2018**, 28, 285.
- [23] J. Deprest, L. Gucciardo, P. Eastwood, S. Zia, J. Jimenez, F. Russo, F. Lesage, L. Lewi, M. Sampaolesi, J. Toelen, *Eur. J. Pediatr. Surg.* **2014**, 24, 270.
- [24] H. R. Davari, M. B. Rahim, N. Tanideh, M. Sani, H. R. Tavakoli, A. R. Rasekhi, A. Monabati, O. Koohi-Hosseinabadi, S. Gholami, *Interact. Cardiovasc. Thorac. Surg.* **2016**, 23, 623.
- [25] R. Langer, J. P. Vacanti, *Tissue Eng. Sci.* **1993**, 260, 920.
- [26] K. M. Brouwer, H. R. Hoogenkamp, W. F. Daamen, T. H. van Kuppevelt, *Am J. Respir. Crit. Care Med.* **2013**, 187, 468.
- [27] K. M. Brouwer, P. van Rensch, V. E. Harbers, P. J. Geutjes, M. J. Koens, R. M. Wijnen, W. F. Daamen, T. H. van Kuppevelt, *J. Tissue Eng. Regener. Med.* **2011**, 5, 501.
- [28] K. M. Brouwer, R. M. Wijnen, D. Reijnen, T. G. Hafmans, W. F. Daamen, T. H. van Kuppevelt, *Organogenesis* **2013**, 9, 161.
- [29] S. F. Badylak, *Ann. Biomed. Eng.* **2014**, 42, 1517.
- [30] R. Londono, S. F. Badylak, *Ann. Biomed. Eng.* **2015**, 43, 577.
- [31] M. E. Alvarez Fallas, M. Piccoli, C. Franzin, A. Sgro, A. Dedja, L. Urbani, E. Bertin, C. Trevisan, P. Gamba, A. J. Burns, P. De Coppi, M. Pozzobon, *Int. J. Mol. Sci.* **2018**, 19, 1319.

- [32] P. M. Crapo, T. W. Gilbert, S. F. Badylak, *Biomaterials* **2011**, *32*, 3233.
- [33] F. Blaudez, S. Ivanovski, S. Hamlet, C. Vaquette, *Methods* **2020**, *171*, 28.
- [34] M. S. B. Raredon, K. A. Rocco, C. P. Gheorghe, A. Sivarapatna, M. Ghaedi, J. L. Balestrini, T. L. Raredon, E. A. Calle, L. E. Niklason, *BioRes. Open Access* **2016**, *5*, 72.
- [35] A. S. Sotnichenko, R. Z. Nakokhov, E. A. Gubareva, E. V. Kuevda, I. S. Gumenyuk, *Bull. Exp. Biol. Med.* **2018**, *166*, 287.
- [36] D. Boso, E. Carraro, E. Maghin, S. Todros, A. Dedja, M. Giomo, N. Elvassore, P. De Coppi, P. G. Pavan, M. Piccoli, *Biomedicines* **2021**, *9*, 709.
- [37] M. Sesli, E. Akbay, M. A. Onur, *Turk. J. Biol.* **2018**, *42*, 537.
- [38] B. J. Jank, L. Xiong, P. T. Moser, J. P. Guyette, X. Ren, C. L. Cetrulo, D. A. Leonard, L. Fernandez, S. P. Fagan, H. C. Ott, *Biomaterials* **2015**, *61*, 246.
- [39] S. A. Grant, C. R. Deeken, S. R. Hamilton, D. A. Grant, S. L. Bachman, B. J. Ramshaw, *J. Biomed. Mater. Res., Part A* **2013**, *101*, 2778.
- [40] C. R. Deeken, S. L. Bachman, B. J. Ramshaw, S. A. Grant, *J. Mater. Sci.: Mater. Med.* **2012**, *23*, 537.
- [41] M. Piccoli, L. Urbani, M. E. Alvarez-Fallas, C. Franzin, A. Dedja, E. Bertin, G. Zuccolotto, A. Rosato, P. Pavan, N. Elvassore, P. De Coppi, M. Pozzobon, *Biomaterials* **2016**, *74*, 245.
- [42] C. Trevisan, M. E. A. Fallas, E. Maghin, C. Franzin, P. Pavan, P. Caccin, A. Chiavegato, E. Carraro, D. Boso, F. Boldrin, F. Caicci, E. Bertin, L. Urbani, A. Milan, C. Biz, L. Lazzari, P. De Coppi, M. Pozzobon, M. Piccoli, *Stem Cells Transl. Med.* **2019**, *8*, 858.
- [43] K. H. Hillebrandt, H. Everwien, N. Haep, E. Keshi, J. Pratschke, I. M. Sauer, *Transplant. Int.* **2019**, *32*, 571.
- [44] E. Morokov, E. Khramtsova, E. Kuevda, E. Gubareva, T. Grigoriev, K. Lukanina, V. Levin, *Artif. Organs* **2019**, *43*, 1104.
- [45] E. A. Gubareva, E. V. Kuevda, S. S. Dzhimak, A. A. Basov, A. S. Sotnichenko, S. N. Bolotin, I. V. Gilevich, I. S. Gumenyuk, P. Macchiarini, *Dokl. Biochem. Biophys.* **2016**, *467*, 113.
- [46] M. P. Eastwood, W. F. Daamen, L. Joyeux, S. Pranpanus, R. Rynkevich, L. Hympanova, M. W. Pot, D. J. Hof, G. Gayan-Ramirez, T. H. van Kuppevelt, E. Verbeke, J. Deprest, *J. Tissue Eng. Regen. Med.* **2018**, *12*, 2138.
- [47] K. M. Brouwer, W. F. Daamen, N. van Lochem, D. Reijnen, R. M. Wijnen, T. H. van Kuppevelt, *Acta Biomater.* **2013**, *9*, 6844.
- [48] S. Parrinello, I. Napoli, S. Ribeiro, P. Wingfield Digby, M. Fedorova, D. B. Parkinson, R. D. Doddrell, M. Nakayama, R. H. Adams, A. C. Lloyd, *Cell* **2010**, *143*, 145.
- [49] L. Crigler, R. C. Robey, A. Asawachaicharn, D. Gaupp, D. G. Phinney, *Exp. Neurol.* **2006**, *198*, 54.
- [50] Y. Urita, H. Komuro, G. Chen, M. Shinya, R. Saihara, M. Kaneko, *Pediatr. Surg. Int.* **2008**, *24*, 1041.
- [51] Z. S. Wu, S. B. Zhang, M. M. Guo, C. R. Chen, G. L. Shen, R. Q. Yu, *Anal. Chim. Acta* **2007**, *584*, 122.
- [52] S. Mayer, H. Decaluwe, M. Ruol, S. Manodoro, M. Kramer, H. Till, J. Deprest, *PLoS One* **2015**, *10*, e0132021.
- [53] K. M. Brouwer, W. F. Daamen, H. R. Hoogenkamp, P. J. Geutjes, I. de Blaauw, W. Janssen-Kessels, W. de Boode, E. Versteeg, R. M. Wijnen, W. F. Feitz, M. Wijnen, T. H. van Kuppevelt, *J. Biomed. Mater. Res., Part B* **2014**, *102*, 756.
- [54] H. F. Shieh, C. D. Graham, J. A. Brazzo 3rd, D. Zurakowski, D. O. Fauza, *J. Pediatr. Surg.* **2017**, *52*, 1010.
- [55] S. M. Kunisaki, J. R. Fuchs, A. Kaviani, J. T. Oh, D. A. LaVan, J. P. Vacanti, J. M. Wilson, D. O. Fauza, *J. Pediatr. Surg.* **2006**, *41*, 34.
- [56] J. R. Fuchs, A. Kaviani, J. T. Oh, D. LaVan, T. Udagawa, R. W. Jennings, J. M. Wilson, D. O. Fauza, *J. Pediatr. Surg.* **2004**, *39*, 834.
- [57] X. Y. Zhang, Y. Yanagi, Z. Sheng, K. Nagata, K. Nakayama, T. Taguchi, *Biomaterials* **2018**, *167*, 1.
- [58] I. Talon, A. Schneider, V. Ball, J. Hemmerle, *J. Surg. Res.* **2020**, *251*, 254.
- [59] C. R. Deeken, D. B. Fox, S. L. Bachman, B. J. Ramshaw, S. A. Grant, *J. Biomed. Mater. Res., Part B* **2011**, *97*, 334.
- [60] Z. Wang, H. Liu, W. Luo, T. Cai, Z. Li, Y. Liu, W. Gao, Q. Wan, X. Wang, J. Wang, Y. Wang, X. Yang, *J. Tissue Eng.* **2020**, *11*, 2041731420974861.
- [61] G. S. Krishnakumar, S. Sampath, S. Muthusamy, M. A. John, *Mater. Sci. Eng., C* **2019**, *96*, 941.
- [62] M. T. Conconi, S. Bellini, D. Teoli, P. de Coppi, D. Ribatti, B. Nico, E. Simonato, P. G. Gamba, G. G. Nussdorfer, M. Morpurgo, P. P. Parnigotto, *J. Biomed. Mater. Res., Part A* **2009**, *89*, 304.
- [63] R. W. Ten Broek, S. Grefte, J. W. Von den Hoff, *J. Cell. Physiol.* **2010**, *224*, 7.
- [64] D. J. Prockop, J. Y. Oh, *Mol. Ther.* **2012**, *20*, 14.
- [65] S. M. Kunisaki, *Stem Cells Transl. Med.* **2018**, *7*, 767.
- [66] L. Wen, M. Zhu, M. C. Madigan, J. You, N. J. King, F. A. Billson, K. McClellan, G. Sutton, C. Petsoglou, *PLoS One* **2014**, *9*, e101841.
- [67] E. J. Grethel, R. A. Cortes, A. J. Wagner, M. S. Clifton, H. Lee, D. L. Farmer, M. R. Harrison, R. L. Keller, K. K. Nobuhara, *J. Pediatr. Surg.* **2006**, *41*, 29.
- [68] R. L. Moss, C. M. Chen, M. R. Harrison, *J. Pediatr. Surg.* **2001**, *36*, 152.
- [69] K. P. Lally, M. S. Paranka, J. Roden, K. E. Georgeson, J. M. Wilson, C. W. Lillehei, C. W. Breaux, Jr., M. Poon, R. H. Clark, J. B. Atkinson, *Ann. Surg.* **2007**, *120*, e651.
- [70] R. L. Romao, A. Nasr, P. P. Chiu, J. C. Langer, *J. Pediatr. Surg.* **2012**, *47*, 1496.
- [71] K. J. Riehle, D. K. Magnuson, J. H. Waldhausen, *J. Pediatr. Surg.* **2007**, *42*, 1841.
- [72] C. A. Laituri, C. L. Garey, P. A. Valusek, F. B. Fike, A. J. Kaye, D. J. Ostlie, C. L. Snyder, S. D. St Peter, *Eur. J. Pediatr. Surg.* **2010**, *20*, 363.
- [73] I. C. Mitchell, N. M. Garcia, R. Barber, N. Ahmad, B. A. Hicks, A. C. Fischer, *J. Pediatr. Surg.* **2008**, *43*, 2161.
- [74] S. A. Steigman, J. T. Oh, N. Almendinger, P. Javid, D. LaVan, D. Fauza, *J. Pediatr. Surg.* **2010**, *45*, 1455.
- [75] S. B. Kang, J. L. Olson, A. Atala, J. J. Yoo, *Tissue Eng., Part A* **2012**, *18*, 1912.
- [76] V. Agrawal, B. N. Brown, A. J. Beattie, T. W. Gilbert, S. F. Badylak, *J. Tissue Eng. Regen. Med.* **2009**, *3*, 590.
- [77] V. Aarimaa, M. Kaariainen, S. Vaittinen, J. Tanner, T. Jarvinen, T. Best, H. Kalimo, *Neuromuscular Disord.* **2004**, *14*, 421.
- [78] J. T. Ross, N. E. Liang, A. S. Phelps, A. I. Squillaro, L. T. Vu, *Front. Pediatr.* **2021**, *9*, 707052.
- [79] M. Quarta, M. Cromie, R. Chacon, J. Blonigan, V. Garcia, I. Akimenko, M. Hamer, P. Paine, M. Stok, J. B. Shrager, T. A. Rando, *Nat. Commun.* **2017**, *8*, 15613.
- [80] J. W. Duess, E. M. Zani-Ruttenstock, M. Garriboli, P. Puri, A. Pierro, M. E. Hoellwarth, *Pediatr. Surg. Int.* **2015**, *31*, 465.
- [81] The Congenital Diaphragmatic Hernia Study Group, *Pediatrics* **2007**, *120*, 651.
- [82] K. Arai, D. Murata, S. Takao, A. R. Verissimo, K. Nakayama, *PLoS One* **2020**, *15*, e0230428.
- [83] L. R. Putnam, K. Tsao, K. P. Lally, M. L. Blakely, T. Jancelewicz, P. A. Lally, M. T. Harting, *J. Am. Coll. Surg.* **2017**, *224*, 416.
- [84] Y. Zhu, Y. Wu, Q. Pu, L. Ma, H. Liao, L. Liu, *Hernia* **2016**, *20*, 297.
- [85] J. Tsai, J. Sulkowski, N. S. Adzick, H. L. Hedrick, A. W. Flake, *J. Pediatr. Surg.* **2012**, *47*, 637.
- [86] M. A. Verla, C. C. Style, T. C. Lee, A. D. Menchaca, P. E. Lau, A. R. Mehollin-Ray, C. J. Fernandes, S. G. Keswani, O. O. Olutoye, *J. Pediatr. Surg.* **2022**, *57*, 637.
- [87] H. L. Short, M. S. Clifton, K. Arps, C. Travers, J. Loewen, A. Schlager, *J. Laparoendosc. Adv. Surg. Tech.* **2018**, *28*, 476.
- [88] C. R. Deeken, A. K. White, S. L. Bachman, B. J. Ramshaw, D. S. Cleveland, T. S. Loy, S. A. Grant, *J. Biomed. Mater. Res., Part B* **2011**, *96*, 199.

- [89] R. B. Raney, J. R. Anderson, R. J. Andrassy, W. M. Crist, S. S. Donaldson, H. M. Maurer, *J. Pediatr. Hematol./Oncol.* **2000**, *22*, 510.
- [90] A. Naik, M. Griffin, M. Szarko, P. E. Butler, *Artif. Organs* **2020**, *44*, 178.
- [91] A. R. Gillies, L. R. Smith, R. L. Lieber, S. Varghese, *Tissue Eng., Part C* **2011**, *17*, 383.
- [92] A. Marg, H. Escobar, N. Karaiskos, S. A. Grunwald, E. Metzler, J. Kieshauer, S. Sauer, D. Pasemann, E. Malfatti, D. Mompoin, S. Quijano-Roy, A. Boltengagen, J. Schneider, M. Schulke, S. Kunz, R. Carlier, C. Birchmeier, H. Amthor, A. Spuler, C. Kocks, N. Rajewsky, S. Spuler, *Nat. Commun.* **2019**, *10*, 5776.
- [93] A. Marg, H. Escobar, S. Gloy, M. Kufeld, J. Zacher, A. Spuler, C. Birchmeier, Z. Izsvak, S. Spuler, *J. Clin. Invest.* **2014**, *124*, 4257.
- [94] D. Moher, L. Shamseer, M. Clarke, D. Ghersi, A. Liberati, M. Petticrew, P. Shekelle, L. A. Stewart, P. - P. Group, *Syst. Rev.* **2015**, *4*, 1.
- [95] C. R. Hooijmans, M. M. Rovers, R. B. de Vries, M. Leenaars, M. Ritskes-Hoitinga, M. W. Langendam, *BMC Med. Res. Methodol.* **2014**, *14*, 43.
- [96] P. E. Bourguine, B. E. Pippenger, A. Todorov, Jr., L. Tchang, I. Martin, *Biomaterials* **2013**, *34*, 6099.
- [97] K. Xu, L. A. Kuntz, P. Foehr, K. Kuempel, A. Wagner, J. Tuebel, C. V. Deimling, R. H. Burgkart, *PLoS One* **2017**, *12*, e0171577.
- [98] E. E. Friedrich, S. T. Lanier, S. Niknam-Bienia, G. A. Arenas, D. Rajendran, J. A. Wertheim, R. D. Galiano, *J. Tissue Eng. Regener. Med.* **2018**, *12*, e1704.
- [99] C. R. Butler, R. E. Hynds, C. Crowley, K. H. Gowers, L. Partington, N. J. Hamilton, C. Carvalho, M. Plate, E. R. Samuel, A. J. Burns, L. Urbani, M. A. Birchall, M. W. Lowdell, P. De Coppi, S. M. Janes, *Biomaterials* **2017**, *124*, 95.



Agnes K. Boehm is a Doctoral Student at Experimental Surgery, Department of Surgery, Charité – Universitätsmedizin Berlin and funded by the BIH MD Student Research Stipend. She pursues her scientific interest in tissue engineering with research on diaphragmatic decellularization and recellularization within the research group lead by Igor M. Sauer and Karl H. Hillebrandt.



Marco N. Andreas is a Clinician Scientist at Experimental Surgery, Department of Surgery, Charité – Universitätsmedizin Berlin and part of the research group led by Igor M. Sauer and Karl H. Hillebrandt. His research focuses on diaphragmatic de- and recellularization, its characterization and translation into clinical applications.



Karl H. Hillebrandt is a Junior Research Group Leader at Experimental Surgery, Department of Surgery, Charité – Universitätsmedizin Berlin and Fellow at the BIH/Charité Clinician Scientist Program. His research focuses on de- and recellularization of tissues as well as organs. Furthermore, his group is specialized on the characterization of decellularized tissues and on the development of new matrix-based models.